

## TABLE OF CONTENTS

<b>CHAPTER 1</b> .....	<b>1</b>
INTRODUCTION .....	1
1.1 Historical Introduction .....	1
1.2 Fundamentals of Superconductivity .....	2
1.3 Advantages of MgB <sub>2</sub> .....	4
1.4 The Mechanism of Superconductivity in MgB <sub>2</sub> .....	5
1.5 The Objective of This Thesis .....	6
<b>CHAPTER 2</b> .....	<b>8</b>
THE CRYSTAL STRUCTURE OF MgB <sub>2</sub> AND PREPARATION OF BULK SAMPLES .....	8
2.1 The Crystal Structure .....	8
2.2 Preparation of Bulk Samples .....	13
Powder blending and consolidation: .....	15
Squeeze casting and squeeze infiltration: .....	15
2.3 Powder In Tube Method .....	16
2.4 Effect of Substitutions on Superconducting Properties of MgB <sub>2</sub> .....	22
2.5 Effect of Pressure .....	25
2.6 Effect of Sintering .....	25
<b>CHAPTER 3</b> .....	<b>28</b>
EXPERIMENTAL METHODS.....	28
3.1 Sample Preparation .....	28
3.2 Measurements .....	31
3.2.1 Four Point Probe Method.....	32
3.2.2 DC Resistance Measurements.....	33
<b>CHAPTER 4</b> .....	<b>35</b>
RESULTS AND DISCUSSIONS .....	35
4.1 Resistivity Results.....	43
<b>CHAPTER 5</b> .....	<b>61</b>
CONCLUSIONS .....	61
<b>APPENDIX</b> .....	<b>64</b>
<b>REFERENCES</b> .....	<b>66</b>

## CHAPTER 1

### INTRODUCTION

Energy demand in modern civilization of 20<sup>th</sup> and 21<sup>st</sup> century has been abruptly increasing with the population growth and attitude of human beings toward consumption. While avalanche of researches have been conducted to find feasible new energy sources, the efficient use of existing ones gains importance. One of the most outstanding solution is employment of superconducting power cables which transport electrical current without any losses. In future, the superconductors will replace most of the power transmission lines. Energy storage and electronics are two other application fields. The wide spread commercial use of present superconducting materials are limited because of their high cost and technical problems. In attempts to obtain superconductors operating at room temperature and qualified for technological applications, new improvements have repercussion in physics as in the case of MgB<sub>2</sub>.

#### 1.1 Historical Introduction

The first observation of superconductivity (Onnes, 1911) phenomenon by Kamerling Onnes in 1911 evoked new enthusiasm in physics. This progress was a product of cumbersome efforts due to very low transition temperature of the first superconducting material, mercury. The transition of mercury from normal state to superconducting state was obtained at 4.2 K. At the beginning of 20<sup>th</sup> century, even it was a separate research field to attain such a low temperature around 4 K and become possible only after the liquefaction of He by Kamerling Onnes with his coworkers. The first superconductors were elements with extremely low transition temperature,  $T_c$ . Nowadays as a result of conducted research, it has been shown that several more compounds behave as superconductor under certain characteristic critical temperature. In addition to the discovery of superconductivity, Kamerling Onnes also suggested a way to carry superconductivity though practice by design of very powerful magnets. In an attempt to achieve that purpose, he used a Ni alloy coated with Pb-rich superconductor solder. The contrary to his expectation, he was only able to achieve superconductivity up to 500 mT and explained his failure with defects in the wire (Kunzler et al., 1961). Unfortunately

due to the magnetic behavior of the superconductors was seriously miscomprehended, the superconductivity research was not progressive enough to trigger a flurry of application for the following 50 years. (Labalester et al., 2001a)

Even though the interest in superconductors decreased significantly in the beginning of the second half of the 20<sup>th</sup> century, in 1961 achievement of high critical current densities under a magnetic field of 8.8 T for Nb<sub>3</sub>Sn at 4.2 K (Kunzler et al., 1961) was an important step. Since liquid nitrogen is almost ten times cost efficient than liquid He, in 1987, the discovery of high temperature superconductors (HTSCs) (Wu et al., 1987) by a transition temperature above liquefaction of nitrogen at 77 K enhanced curiosity in that field. When ease of reach to 12 K by use of compressors without cryogenics is concerned, that was an important achievement.

Recent observation of superconductivity around 39 K in a simple intermetallic compounds MgB<sub>2</sub> by Akimitsu and his colleagues (Namatsu et al., 2001) resuscitates studies again. This discovery was announced by Akimitsu at a conference in Sendai, Japan in early January 2001. MgB<sub>2</sub> is a known material since early 1950's but only at 2001 it is revealed that MgB<sub>2</sub> is a superconducting material. In two years, a lot of experimental and theoretical studies have been performed to understand the nature of superconductivity in this material.

## **1.2 Fundamentals of Superconductivity**

When the temperature is lowered, the resistivity of metals gets smaller and smaller and eventually reaches a constant value. In some metals, the resistance does not vanish as the temperature approaches 0 K. This is due to scattering of electrons by imperfections and impurities found in the lattice. However, this is not the case for all kind of materials. Materials through which resistance to electric current disappear under a certain critical temperature ( $T_c$ ) are called as superconductors. Here the critical temperature is defined as the temperature below which a superconductor exhibits superconductivity at zero magnetic field strength and without transporting any current. These materials are in normal state above the critical temperature and in the normal state, they generally have rather poor conductivity. Gold, silver and copper do not superconduct. Ideally, when a supercurrent circulates on a closed loop of a superconductor, the electrons are never dumped. In spite of impurities and imperfections, the current in the loops lasts for a long course of time. An experiment

performed by Collins in 1959 exhibited that no observable decrease occurred two and half year after the induction of current around such a superconducting ring (Tinkham, 1975). In addition, File and Mills performed an experiment by use of precision nuclear magnetic resonance method and as a result of experiments they claim that supercurrents in a solenoid last more than 100,000 years (File et al., 1963).

Superconductors are in demand for technological applications on account of not only almost vanishing resistance of them but also magnetic properties as mentioned above. Until some characteristic magnetic field ( $H_c$ ) superconductors excludes magnetic field lines. If a magnet is placed above a superconductor and cooled below its transition temperature, the magnet levitates. This effect of superconductors was first observed by Meissner and Ochsenfeld and is called as Meissner effect. Magnetic levitation trains (MAGLEVS) are an application of this effect.

Superconductors classified in to two groups as type I and type II with respect to their magnetic behavior. If the whole material completely transforms from normal state to superconducting state under critical temperature and field, it is called as type I. On the other hand, if this transition occurs partially between upper and lower critical field with formation of mixed state, this kind of material is included in the type II class. The mixed state is formed by the existence of both superconducting and normal states together in the same material. These cases in the material occur via formation of vortices, swirling tubes of electrical current induced by an external magnetic field into the surface of a superconducting material. Superconductivity is completely suppressed within these regions. When a current passed through a superconductor in mixed state because of Lorentz Forces and resulting dissipation of energy the vortices are exposed a resistance at right angles to the current flow. (Bishop et al., 1993). The pseudo-resistance resulted from the motion of this volcano shaped structures are undesirable and can be overwhelmed by introducing pinning centers about which more mentioned later.

While type I superconductors are elements and not appropriate for technological applications resulting from their low  $H_c$  values, type II superconductors (Feng et al., 2002) are compounds and complex materials with wide area of applications. The upper critical field of type II is much larger than that of type I superconductors. This property is sufficient to extinguish these two classes from each other. Type II superconductors are good candidate materials for magnet applications because of their large upper-critical fields.  $MgB_2$  takes part in type II superconductors and as mentioned above

pinning center play an important role in the electrical conduction properties of the material.

### **1.3 Advantages of MgB<sub>2</sub>**

The highest transition temperature for conventional alloys and metals was 23 K before the discovery of MgB<sub>2</sub>. This value was first attained by Nb<sub>3</sub>Ge in 1973 and then one year after by a Y-Pd-B-C compound. According to the present indications MgB<sub>2</sub> promises higher device speeds and higher operating temperature than the already existing electronics based on Nb (Buzea et al., 2001). The MgB<sub>2</sub> bulk material presents several major advantages both with respect to the low temperature superconductors and with respect to the higher temperature superconductors based on cuprates. The major advantage of MgB<sub>2</sub> relative to NbTi and Nb<sub>3</sub>Sn is the use of a refrigeration system without cryogenic liquid He (Giunchi et al., 2002). In addition, as reported by Larbalestier et al. in 2001b, the grain connectivity, which means having a link or small distance between grains, associated with MgB<sub>2</sub> is as good as in Nb<sub>3</sub>Sn.

Although MgB<sub>2</sub> has relatively low T<sub>c</sub> with respect to HTSCs, it has drawn remarkable attention. The reason of this aroused interest can be interpreted as follows: HTSCs are anisotropic in structure and have low critical current densities in long range because of problem in grain connectivity. Furthermore they are very brittle in structure and sensitive to elemental substitutions. By using Ag as cladding materials, they gain ductility. However, this increases cost in applications like tapes and cables. As a result of good grain connectivity in MgB<sub>2</sub> (Larbalestier et al, 2001b) and large coherence lengths relative to HTSCs, the weak links do not form a major concern in the superconductive properties of MgB<sub>2</sub>. The coherence length in it is shown to be longer than that in the HTSC cuprates (Finmore et al., 2001). It is about 5.2 nm (Finmore et al., 2001). The supercurrents in MgB<sub>2</sub> show stability with time (Thompson et al., 2001). MgB<sub>2</sub> can be obtained either by reliable rapid synthesis or as commercially available powders. These advantages made this material suitable for commercial applications. Although MgB<sub>2</sub> is also brittle material, it is possible to increase the ductility and malleability of MgB<sub>2</sub> by using cladding materials or fabricating composites. In the selection of materials the effect of elemental substitutions on the superconducting properties of MgB<sub>2</sub> and relatively low decomposition and melting temperature should

be concerned. The substitutions may increase or decrease superconducting properties of  $\text{MgB}_2$ . They may play role as pinning center and concomitantly increase the  $J_c$ .

#### **1.4 The Mechanism of Superconductivity in $\text{MgB}_2$**

From some aspects (Choi et al., 2002),  $\text{MgB}_2$  is different than ordinary metallic superconductors. The conventional models (Eliashberg, 1960) cannot predict very high transition temperatures such as 40 K. On the other hand, as a result of band structure studies, observation of isotope effect and some related works, it is generally classified as a conventional BCS type superconductor (Choi et al., 2002). BCS type superconductors are materials of which microscopic theory was founded in 1957-1958 by J. Bardeen, L. Cooper, J. Schrieffer. Now this theory is referred as BCS theory. According to the BCS theory, the superconductivity occurs via pairing of electrons as a result of attractive interaction between electrons, mediated by lattice vibrations, phonons. BCS theory is appropriate for the weak-coupling (the strength of coupling with phonon vibrations and electrons) limit and in the strong coupling limit a more general form of it found by Eliashberg is valid (Eliashberg, 1960).

$\text{MgB}_2$  shows superconductivity at a temperature ~33% higher than the theory seemed to allow (Brumfiel, 2001). To explain such a high transition temperature, several attempts and suggestions were made.  $\text{MgB}_2$  might have come from a new class of superconductors or since  $\text{MgB}_2$  has a structure with alternating layer of Mg atoms and honeycomb boron layers, as anticipated by BCS theory the light boron atoms might have been a reason for high  $T_c$  in  $\text{MgB}_2$  (Kortus et al., 2001; Bud'ko et al., 2001).

In the summer of 2001, two independent studies were published (Osborn et al., 2001; Yıldırım et al., 2001). In one of the studies, Osborn and his group reported inelastic neutron scattering measurements of phonon density of states on an isotopically enriched polycrystalline sample of  $\text{Mg}^{11}\text{B}_2$  prepared at Argonne National Laboratory (Osborn et al., 2001). This study determined the lattice vibration energies and allowed them to conclude that superconductivity is consistent with a conventional phonon mechanism with moderately strong electron-phonon coupling.

The other study was conducted by a collaboration led by Jeff Lynn and Taner Yıldırım of National Institute of Standards and Technology in Gaithersburg confirms the Argonne group's neutron scattering results and proposes a more detailed analysis using a model of  $\text{MgB}_2$  based on the fundamental laws of superconductivity (Brumfiel, 2001).

According to the study, there are four phonon modes in the zone center, three of these modes are harmonic up to  $u/a \approx 0.065$  ( $u$  is magnitude of the displacement of ions with phonon vibration and  $a$  is the lattice constant) one of them is very inharmonic. They calculated an insignificant coupling for three harmonic modes and concluded that electron-phonon coupling is negligible for these modes. However, for the inharmonic mode, the coupling is large indicating significant non-linear electron phonon coupling. In this mode, the boron ions vibrate in opposite directions. After the calculation, they infer that  $\text{MgB}_2$  is a conventional electron-phonon superconductor in the strong regime and the conducting electrons form pairs by connecting to each other via specific lattice vibrations. (Yıldırım et al., 2001) The pair formation can be simply explained with regard to inharmonic mode. In this mode, boron ions vibrate in opposite directions along  $x$  (or  $y$ ) axis, with the Mg ions stationary, when two boron atoms become close enough electrons are let to jump between them. As a consequence of the correlation between lattice vibrations and electrons cooper pairs and enormous vibrations are formed. (Yıldırım et al., 2001; Brumfiel, 2001)

After the detailed theoretical studies given above the material properties, the strong coupling formalism of superconductivity, and the reproduction of superconducting transition temperature of  $\text{MgB}_2$  become possible (Choi et al., 2002).

### **1.5 The Objective of This Thesis**

Concerning the brittle structure and interruption of the superconducting phases by cracks, the widespread use of  $\text{MgB}_2$  in applications becomes possible with increasing the ductility of  $\text{MgB}_2$  by use of malleable metals. One way for rendering  $\text{MgB}_2$  with improved mechanical properties is the production of composites as previously touched on. The melting point of  $\text{MgB}_2$  is 1073 K and decomposition temperature is above that value. (Sharoni et al., 2001) To form composites, one should select a metal with lower melting temperature.  $\text{MgB}_2$  composites with Al, Mg and Zn were fabricated and found that their transition temperatures around 37 K. In spite of an observed reduction in the  $\text{MgB}_2$  transition temperature by an amount of 2 K, it is still much higher than existing conventional superconductors. Among these three metals, composites synthesized by Mg have highest critical current density,  $5.6 \times 10^5 \pm 5.6 \times 10^4 \text{ A/cm}^2$  (Dunand a).

In this study, we have chosen Mg among the candidate materials to fabricate metal matrix composites of  $\text{MgB}_2$ . The reason for this choice is that Mg undergoes no reaction

with  $\text{MgB}_2$  and has relatively low melting point. Furthermore, excess Mg might help  $\text{MgB}_2$  to keep stoichiometry. The commercially available  $\text{MgB}_2$  powders (98% pure) manufactured by Alfa-Aesar are used in the fabrication of Mg/ $\text{MgB}_2$  metal matrix alloys. To measure the  $T_c$  of Mg/ $\text{MgB}_2$  metal matrix composites, we have performed standard four-probe dc resistivity method. In addition, structural characterization has been made by X-Ray Diffraction and Energy Dispersive Spectroscopy (EDX).

## CHAPTER 2

### THE CRYSTAL STRUCTURE OF $\text{MgB}_2$ AND PREPARATION OF BULK SAMPLES

#### 2.1 The Crystal Structure

The existence of  $\text{MgB}_2$  was first revealed at early 1950's but superconducting behavior of it first observed in 2001. As mentioned in the first chapter, the metallic conventional superconductors have many advantages compared  $T_c$  to high temperature superconductor cuprates and the discovery was striking because  $\text{MgB}_2$  was almost doubling  $\text{Nb}_3\text{Ge}$  in transition temperature. Before  $\text{MgB}_2$  the highest  $T_c$  among binary metallic compounds was just 23 K, which is the transition temperature of  $\text{Nb}_3\text{Ge}$ .

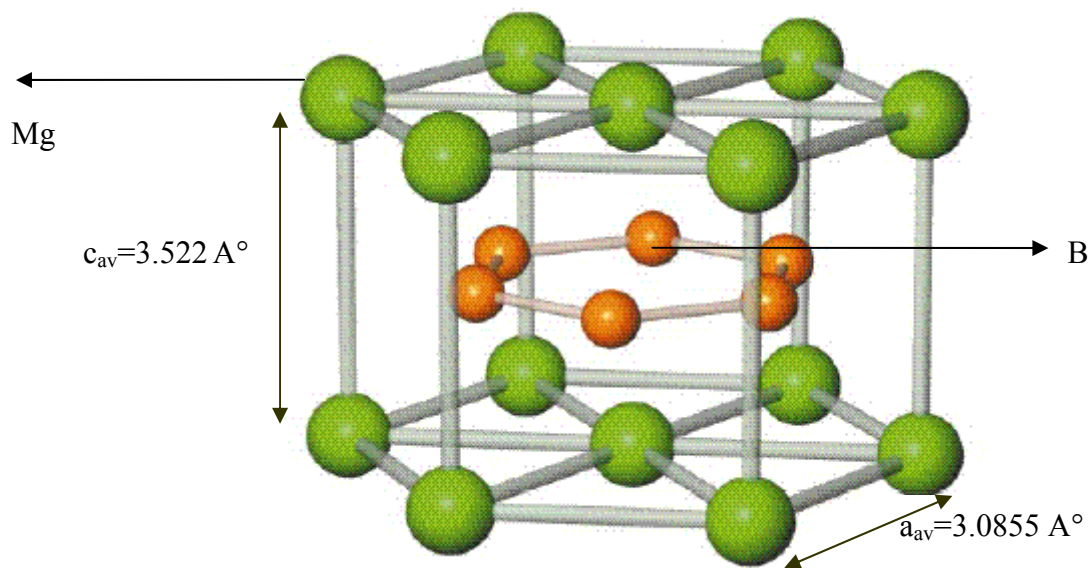


Figure 2.1 The structure of  $\text{MgB}_2$  (Larbalestier et al., 2001)

The structure  $\text{MgB}_2$  suits that of simple hexagonal  $\text{A}_1\text{B}_2$ -Type materials. Close-packed layers of magnesium are sandwiched between honeycombs like boron layers. As seen in the Figure 2.1 magnesium atoms are located at the midpoint of boron hexagons. The lattice constants  $a$  and  $c$  of  $\text{MgB}_2$  change with the starting composition of Mg and B. With different starting compositions the values of  $a$  and  $c$  become  $3.0855 \pm 0.0006 \text{ \AA}$  and  $3.522 \pm 0.002 \text{ \AA}$ , respectively. Since variations in the values of  $c$  are larger than the

statistical errors and probably caused by random instrumental errors, in the study these were partially overwhelmed by simply taking  $c/a$  ratio. In average  $c/a$  is equal to 1.1414 and since the changes in the  $c$  values 3.5 time greater than that of  $a$ ,  $c/a$  mainly shows the change in the  $c$  axis.

The results obtained from the calculations made on the band structure of  $\text{MgB}_2$  give signs of the substantial ionization of Mg by wholly transferring the electrons founding 3s orbital to 2 dimensional boron sheets (Kortus et al., 2001; Buzea et al., 2001). Hence, ionic Mg-B bonds and covalent B-B bonds forms the hexagonal structure of  $\text{MgB}_2$  (Kortus et al.; 2001; Tampari et al., 2002). As a result of the anisotropy in the bond lengths between boron ions found in the same plane and neighboring planes, boron ions in  $\text{MgB}_2$  gain very similar structure to that of graphite. 2 p boron states have metallic character and determine the density of states at the Fermi energy,  $E_f$  which are energy of the highest occupied states at the ground state of a system (An et al., 2001). The Fermi surfaces of  $\text{MgB}_2$  comprise two sheets from the  $\sigma$ -bonding states of boron  $p_{x,y}$  orbitals and two sheets from the  $\pi$ -bonding states of boron  $p_z$  orbitals. The  $\sigma$ -bonding states at the Fermi level derived from boron  $p_{x,y}$  orbital are confined in the boron planes (Choi et al., 2002b). The bands near Fermi level and superconductivity arise mainly from  $2p_{xy}$   $\sigma$  bonding orbital of boron (An et al., 2001). Contrary to the graphite, the  $\sigma$ -bonding states in this structure are partially occupied and the charge in the  $\sigma$ -bonding states are not distributed symmetrically relative to the in plane position of the boron atoms (Choi et al, 2002b, T. Yıldırım et al., 2001). In consequence, like in the case of HTSCs,  $\text{MgB}_2$  is a holes-based superconductor (Kang et al., 2001). The unsymmetrical charge distribution in the  $\sigma$ -bonding states leads the only strong coupling in the Fermi level and so strong electron-pair formation. In comparison with  $\sigma$ -bonding states, the  $\pi$ -bonding states form much weaker pairs. The main contribution to superconductivity comes from the pair formation resulting from the strong-coupled  $\sigma$ -bonding states, confined to the boron planes (Choi et al., 2002b). Contribution of Mg-B ionic bond to the superconductivity is not noticeable (T. Yıldırım et al., 2001). While electron pair formation of  $\sigma$ -bonding states posses an average energy gap  $\Delta = 6.8$  meV that of the  $\pi$ -bonding states has only an average 1.8 meV (Choi et al, 2002b).

Result of calculations performed according to Eliashberg formalism suggests that superconducting energy gap of  $\text{MgB}_2$  has s-wave symmetry. In s-wave symmetry, even the size of the gap can change drastically on the different parts of the plane, the gap takes non-zero values and posses the same sign everywhere on the Fermi surface.

Notwithstanding conflicting experimental results about the number of gaps in the  $\text{MgB}_2$ , the two-gap structure and their values obtained from the theoretical calculation of  $\Delta$  by Eliassenberg formalism is confirmed with the recent experiments (Choi et al., 2002b).

The isotope-effect (the effect of change in the phonon vibrations and so  $T_c$  due to the different masses of isotopes) coefficient is large for B but quite small for Mg (Hinks et al., 2001, An et al., 2001) with the reduced total coefficient of 0.32 (Hinks et al., 2001). Evidence for a multi-component gap has been obtained from measurements of the specific heat, whose temperature and field dependence are substantially different from that of isotropic s-wave superconductors (T. Yıldırım et al., 2001). The emerging picture is that  $\text{MgB}_2$  has properties resembling that of photon-mediated BCS type conventional superconductor with a more complex nature than existing ones.

There are several attempts to obtain nonstoichiometric compositions of  $\text{MgB}_2$ . Only a few try leads to significant substitutions on the either sites. While in many studies nonstoichiometry is speculated as explanation of variation in the different samples prepared at the same synthesis temperature with a range of composition, it is revealed that  $\text{MgB}_2$  is a line compound (Ribeiro et al., 2002). In the study,  $\text{Mg}_x\text{B}_2$  was produced by different starting compositions ranging between  $x=0.6$  and  $x=1.3$ . According to this study excess Mg exist as an impurity phase in Mg rich region. The researchers hypothesized that some of the Mg is situated on the grain boundaries. For higher concentrations of Mg than that in  $\text{Mg}_{1.1}\text{B}_2$ , Mg leads to relieve of the interaction among the randomly oriented  $\text{MgB}_2$  crystals. When composition is in between  $\text{Mg}_{0.9}\text{B}_2$  and  $\text{Mg}_{1.1}\text{B}_2$ , the amount of Mg metal or  $\text{MgB}_4$  impurities are not significant to dominate the behavior of the lattice and it is mainly determined by grain interaction stresses among the randomly oriented  $\text{MgB}_2$  crystals. When  $x$  is less than 0.9 the concentration of  $\text{MgB}_4$  impurity phase becomes important in the behavior of the material. In that case the response of the lattice and peak broadening parameters influenced by both  $\text{MgB}_2$  and  $\text{MgB}_4$ , and they behave as  $\text{MgB}_2/\text{MgB}_4$  composites. At the end of the study the researchers conclude that with the given range of starting composition nonstoichiometry is possible with a maximum 1% Mg vacancy in the  $\text{MgB}_2$  structure, the other variations of the composition lead impurity formations in the material. Furthermore they also claim that the behavior of  $T_c$  determined by the impurities in the Mg and B. The accidental impurities in the sample caused by Mg and B can be used to provide

deliberate chemical substitutions like use of BC as starting material to synthesize C-doped  $\text{MgB}_{2-x}\text{C}_x$  (Ribeiro et al., 2002; Hinks et al., 2002).

In the following part XRD analysis of the materials used in our experiments are given. Figure 2.2 shows XRD analysis belongs to the commercially available Alfa Aesar  $\text{MgB}_2$  powders and the Figure 2.3 belongs to the Mg powder. Although they are not denoted in the XRD graph due to their weak peaks search match results indicate that small amounts of  $\text{MgB}_4$  and  $\text{MgB}_6$  phases can exist in the commercially obtained powder.

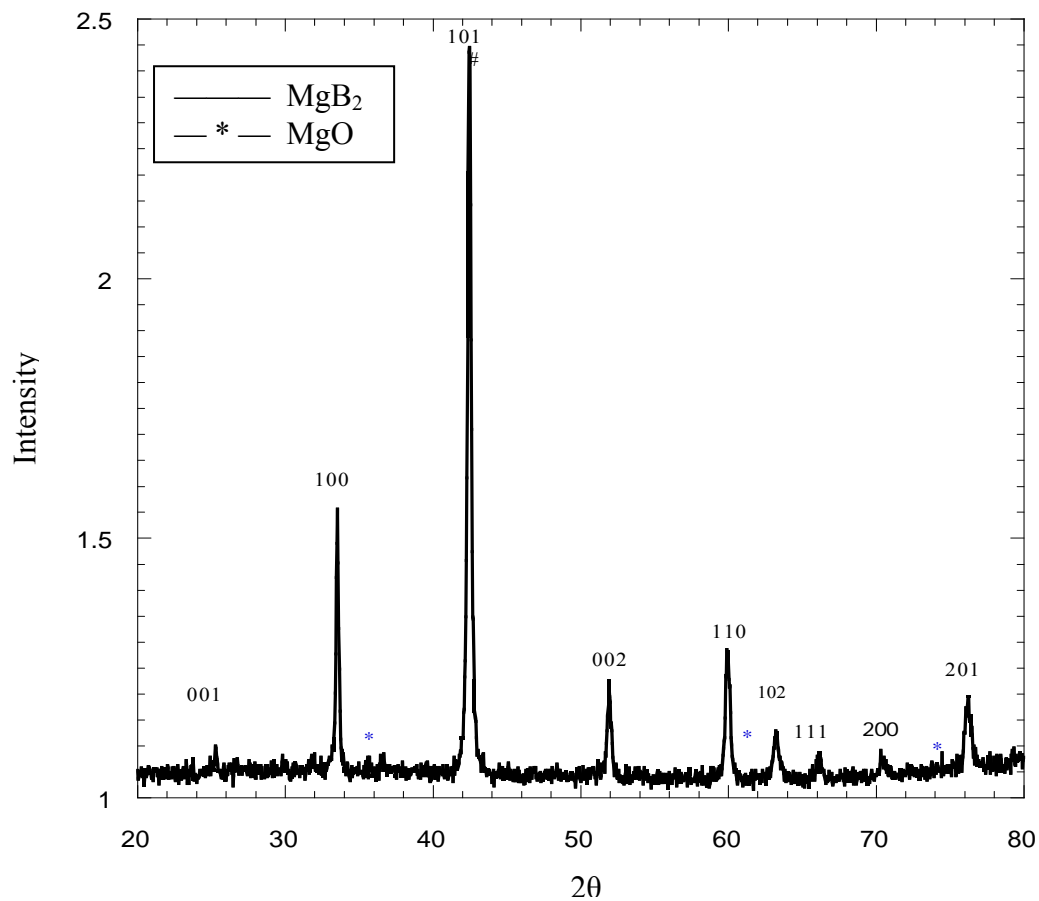


Figure 2.2 XRD Pattern of Commercial  $\text{MgB}_2$

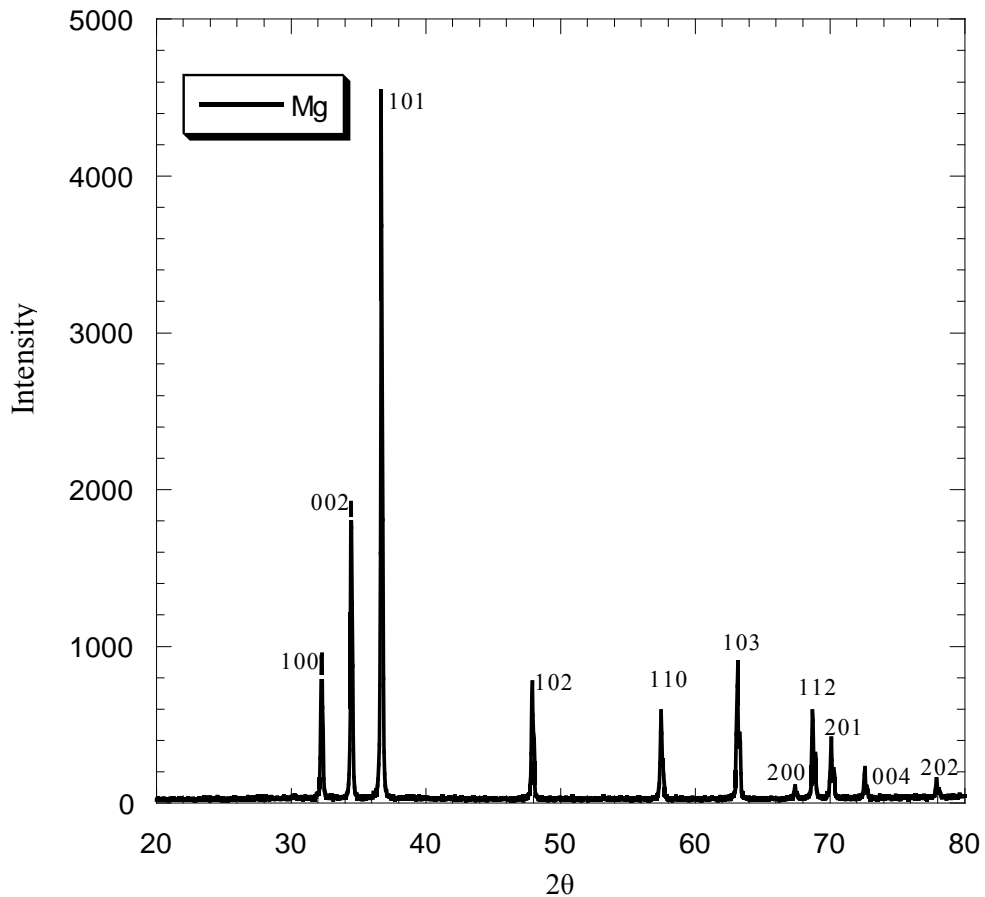
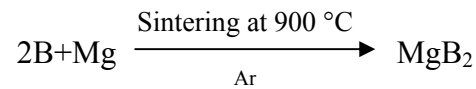


Figure 2.3 XRD Pattern of Mg powder

Mechanical properties of pure  $\text{MgB}_2$  are very poor for application. As a result of this, extensive research has been conducted to increase malleability and ductility of the  $\text{MgB}_2$ . To introduce such properties, one method is the production of tapes, wires or ribbons by use of a metal sheaths and another one is fabrication of composites. There are many factors affecting the superconducting and mechanical properties of  $\text{MgB}_2$  samples, so the techniques used in the preparation of bulk samples are very important and need to be more closely examined.

## 2.2 Preparation of Bulk Samples

Although there are many methods to obtain  $\text{MgB}_2$ , all of them mainly based on the solid-state reaction of B and Mg atoms. The following reaction represents such a formation of  $\text{MgB}_2$ .



There are many factors affecting the quality and cost of the resultant  $\text{MgB}_2$ . Evidently approach followed in production and the quality of initial B and Mg are some of the most important points among them.

To obtain  $\text{MgB}_2$  by the solid-state reaction, initial stoichiometry of Mg and B is not necessary. Starting composition ratio of Mg and B is a factor that alters superconducting properties (Hinks et al., 2002). Even initial nonstoichiometric composition can lead to better results (Schlacher et al., 2002). On the other hand, the role of it is less than the purity of the initial powders (Hinks et al., 2002). One of the major factors affecting the residual resistivity ratio ( $\text{RRR} = \rho(300\text{ K})/\rho(40\text{ K})$ ) and  $\rho_0$  values of  $\text{MgB}_2$  is the purity of the B powders. Especially initial boron powder impurity may result in RRR values as low as 4 and high purity cause RRR values of more than 20 with a residual resistivity  $0.4\ \mu\Omega\text{ cm}$ . In addition,  $T_c$  values slightly increase with increasing purity of B powder (Ribeiro et al., 2002). Non-stoichiometry is possible with 1% Mg vacancy in  $\text{MgB}_2$  excess Mg and  $\text{MgB}_4$  is included in the structure as impurity phases (Hinks et al., 2002).  $T_c$  decreases slightly in the Mg-rich region and no considerable change in the deficient side. This may be a result of impurities in Mg. In another study it is claimed that Mg deficiency causes a decrease in  $T_c$  as much as 3 K with  $x = 0.5$  at  $\text{Mg}_x\text{B}_2$  (Zhao et al., 2001).

Modern practical superconductors are required to exhibit a wide range of properties. To meet these needs a somewhat specialized group of composites with their accompanying fabrication techniques have been innovated. Besides the best properties possessed by the ingredients, the composites even exhibit some extra properties not attainable by either of them. Although there is no absolute definition given by an authority, a more applicable one is that composites are materials containing a mixture of two or more types of fundamentally different components, one of which acting as a matrix (or binder) material completely surrounding the other constituents, namely reinforcements. The combining of two or more materials is done by physical means and

have distinctive component properties, in other words the components are generally mechanically separable and not lose their identity as opposed to chemical bonding occurring in the alloys of monolithic solid materials. In composites mixing occur in macroscopic scale not in atomic scale.

The types of reinforcements used in composites have different effects on the characteristics of the composites. Reinforcements are usually found in the form of fibers, particles or whiskers in the matrix materials. Whiskers are elongated single crystal particles with a definite width-to-length ratio less than one and significantly improved properties. A prior property of the fibers is having one very long axis compared to the others, which are often circular or near circular. While whiskers lengths typically range between 2-50 nm that of fibers are much larger than these values. Some of the whiskers are preferred in ceramic or metal matrix according their capacity to withstanding temperature as high as 2000 °C and some others are used in place of fibers for a better process. Because of additional effort needed to bring on composites including whiskers with desired configuration and their cost, practical uses of them are limited. In the literature, there is a study of microstructure of in-situ formed  $MgB_2$  phases in a hybrid Mg alloy matrix composites reinforced with SiC whiskers and  $B_4C$  particles (Chen et al., 2002). In this study  $MgB_2$  are in-situ formed by the following chemical procedure:  $B_4C + O_2 \rightarrow B_2O_3 + CO_2$ ,  $B_2O_3 + Mg \rightarrow MgB_2 + MgO$ . As a result of reaction the  $MgB_2$  faces obtained with SiC reinforcements. In the structure another benefit of  $B_4C$  particles additional to behaving as boron source for  $MgB_2$  is that they attempt to separate the SiC whiskers uniformly in the composite. Today most of the superconductors in use, are composites. The composites based on the low  $T_c$  materials, NbTi,  $Nb_3Sn$ ,  $Nb_3Ge$ .

Since, we need to improve mechanical and electrical properties of  $MgB_2$ , the metal matrix composites (MMCs) is proper choice and naturally preferred to the other five classes of composites, namely polymer matrix composites (PMC), fiber reinforced plastics (FRP), ceramic matrix composites (CMC), fiber glasses and advanced fiber composites. Due to the subject of this thesis, I will explain only MMC and skip the later five. Numerous fabrication techniques exist for MMCs. Among the candidates two methods namely powder blending and consolidation, and squeeze casting and squeeze infiltration, are main applied methods for the production of the metal/ $MgB_2$  composites.

**Powder blending and consolidation:**

Powder blending and consolidation method is a commonly used method for the preparation of discontinuously reinforced MMCs. Powders of the metallic matrix and reinforcement are first blended and fed into a mold of the desired shape and subsequent to these processes consolidation is performed either by uniaxial hot pressing (UHP) or hot isostatic pressing (HIP) (DDA, 1999; Giunchi et al., 2002). Even by use of these techniques high pressure prevents the decomposition of the  $MgB_2$ , unfortunately the use of both HIP and UHP bring some limitations due to the practical difficulty in the use of very large vessels and dyes, when high pressure and high temperatures are involved (Giunchi et al., 2002).

**Squeeze casting and squeeze infiltration:**

Pressure infiltration, which promotes wetting of fibers by matrix and reduces porosity, is often called squeeze casting. Porous preforms of reinforcement material are infiltrated by molten metal under pressure to produce metal matrix composites. Composites can be made by infiltrating liquid metal into a fabric or prearranged fibrous configuration called a preform. Frequently, ceramic or organic binder materials are used to hold the fibers in position. The latter is burned off before or during infiltration. Infiltration can be carried out under vacuum, pressure, or both. It is shown that obtaining high density and high quality  $MgB_2$  pellets is possible with liquid infiltration technique (Giunchi et al., 2002). In the study porous body of B powders (preforms) is infiltrated with liquid magnesium and densification made possible only by use of metallic container without the standard way of consolidation techniques applied in powder blending method. The inner walls of the container counteract the pressure by the expansion of the  $MgB_2$  forming phase and leads formation of a dense structure. Even in the study one of the best  $J_c$  and applied magnetic field relation obtained for bulk  $MgB_2$ , when compared to the other superconducting materials it is revealed that further improvements such as better flux pinning mechanism improvement is necessary to compete with them (Giunchi et al., 2002).

For MMCs several aspects such as forms and types of the matrix and the reinforcement materials should be take in to consideration to obtain suitable composites for specific applications. Properties of different type of matrix materials like electrical

resistance, melting temperature and strength can dramatically affect the end product characteristics.

A common method to study the factor affecting the properties and improve  $\text{MgB}_2$  for several applications a common method is the fabrication of pellets. To develop a commercial or technologically applicable product many tries are required. Fabrication of pellets provides cost effective and easy method to test several factors. The other objective behind the production of pellets can be summarized as follows:

- By formation of pellets, it is more become to use measurement methods like four probe technique which will be mentioned in the following chapter of this thesis.
- It becomes possible to study effects of several factors easily in a small volume.
- If the pellets are formed to synthesis  $\text{MgB}_2$ , pressure can enhance the formation of  $\text{MgB}_2$  by decreasing the distance between Mg and B powders.
- Increasing grain connectivity: The applied pressure to form pellets decrease distance between grains. If this distance is larger than the coherence length weak link problems occur.

However in practice superconductors generally are not used in the form of pellets. In addition to the requirement for higher values of  $T_c$ ,  $H_c$  and  $J_c$  for a superconductor, from the manufacturing point of view these products must be capable of being economically fabricated with relative ease in to long lengths and with properties, which are invariant along the composites. To perform such a long length superconductors, wires and tapes are produced by cladding of the superconductor materials. The cladding materials need to have high thermal and electrical properties because they provide parallel electrical conduction and thermal stabilization.

### **2.3 Powder In Tube Method**

To produce wire and tapes most applied method is powder in tube (PIT) technique. Wires and tapes should be malleable. To increase this property of commercially available  $\text{MgB}_2$ , stoichiometric or near stoichiometric rates of Mg and B are inserted in to metal clad. PIT method consists in the following procedure:

- $\text{MgB}_2$  reacted powder or a mixture of Mg and B powders packed in various metal tubes or sheaths.
- These tubes are drawn into wires as seen in Fig. 2.4, cold-worked into ribbons, if in-situ formation is preferred a heat treatment around  $950\text{ }^\circ\text{C}$  is required for the

formation of  $\text{MgB}_2$ . Otherwise followed by optional a heat treatment at 900-1000 °C

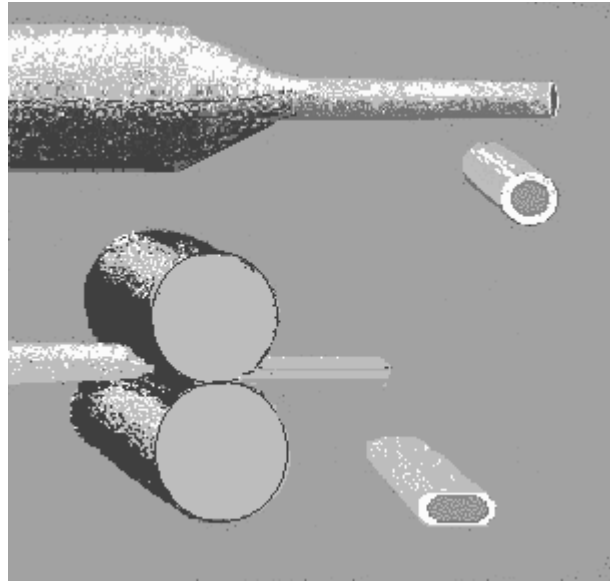


Figure 2.4 A Simple Demonstration of Powder in Tube Method

To fabricate multi-filamentary cables many of this filaments brings together by bundling and further drawing and rolling. The Fig. 2.5 is a cross section of a HTS tape. From top to bottom magnification is increased. The darker parts correspond to superconducting materials, light parts are Ag sheaths. In this structure, the single filaments of superconductors are brought together to form small-cylindrical bundles, then by repeating application of PIT methods the larger bundles were obtained. The application of this method three times, the tape cross-section given at the top of the picture is obtained.

Because of strong chemical reactivity of  $\text{MgB}_2$  the choice of proper metal cladding is a critical point. If sintering is required, many metals, which have low melting points, should be excluded. Even many become useless during the sintering of  $\text{MgB}_2$  around 900-1000 °C due to the tendency of Mg in  $\text{MgB}_2$  to react and combine with many metals by forming solid solutions or intermetallics by lowering the melting points. On the other hand, many inert refractory metals such as Mo, Nb, V, W and Hf are not ductile and malleable enough. As a result of these, only a few materials appeared to be appropriate to use cladding such as Fe, stainless steel and Ti (Jin et al., 2001). Hardness of the core is correlated to sheath materials. The harder the sheath material are used, the harder core obtained (Matsumoto et al., 2002; Kitaguchi et al., 2001).

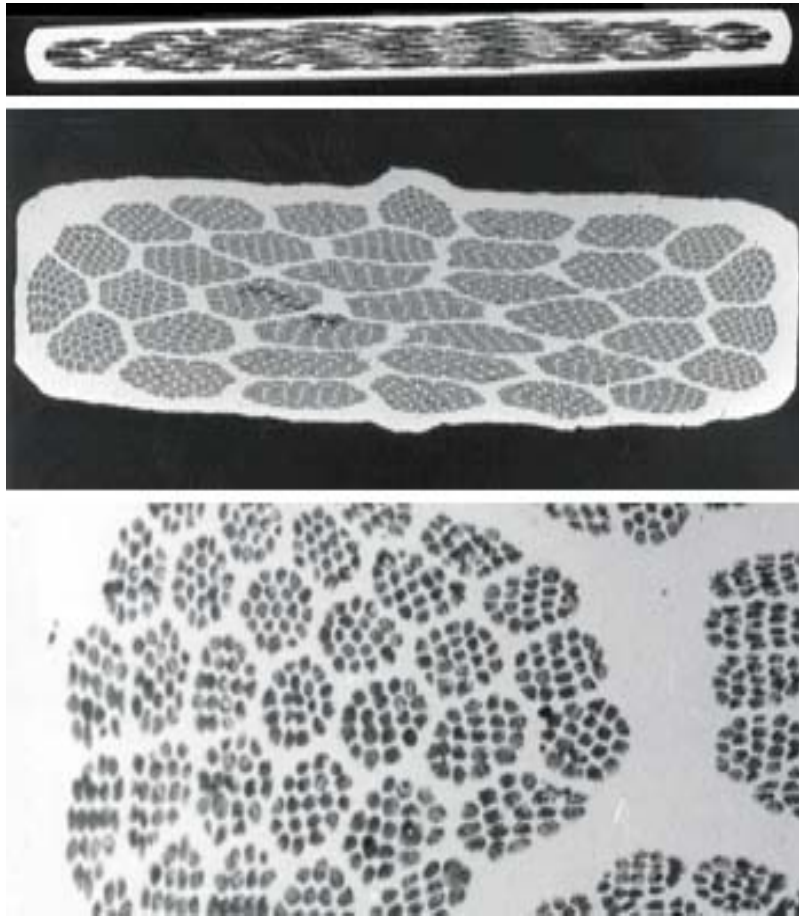


Figure 2.5 The cross-sections of high-temperature superconducting wires (Tallon, 2001)

There are many other factors affecting the performance of the tapes, wires and cables produced by PIT techniques. Each technique leads different microstructural and superconducting properties. A brief summary of the factors affecting superconducting properties take part in the literature is given in the following sections of this chapter.

In an issue, the powder-in-tube process is applied to obtain stainless-steel ribbons, and for sintering and non-sintered ribbons  $T_c$  (onset) values are found as 38.5 and 36 K, respectively. These samples have a sharp superconducting transition. Even the sintering ones have 2.5 K higher transition than that of no-sintering ones, still they have sharper transition and higher  $T_c$  than these of pellets fabricated under 3 GPa (Jung et al., 2001) with commercially available  $MgB_2$  powder without any heat treatment. The improved properties the non-sintered ribbons compared to the pellets can result from swaging and rolling of the tubes (Song et al., 2002).

In-situ and ex-situ formed  $\text{MgB}_2$  wire show different properties. Even though it seems that most outstanding method is the ex-situ fabrication of wire with commercially available homogenous  $\text{MgB}_2$  without any substitutions, the better critical current densities can be obtained by in-situ formation of  $\text{MgB}_2$  (Schlacher et al., 2002). In double heat treated with Fe cladding  $\text{MgB}_2$  wires, non-stoichiometric Mg:B precursor ratio of 0.9:2 shows the best  $J_c$  values for both ex-situ and in-situ wires with 0.7:2 up to 1.3:2 formed wires. Contrary to this, best  $T_c$  values are obtained with loosely packet commercial powder in a sample holder and  $T_c$  values of heat-treated in-situ formed  $\text{MgB}_2$  wires. For both type of the wires, the heat treatment cause an increases in  $J_c$  and  $T_c$  (not much than 40 K) values. In the study, better  $J_c$  values of non-stoichiometric  $\text{MgB}_2$  wire is explained by presence of good percolation paths with Mg precursor sides suppose to contain more Mg than that required for  $\text{MgB}_2$  formation. These parts are situated between the boron rich grains through with little amount of Mg penetrate by dendrite like cracks.

In in-situ fabrication process, the losses of the Mg near the cladding zones must be considered. For example, large solubility of Mg in silver leads wires with rather porous core with decreased superconducting properties (Matienez et al., 2002). After the most of the Mg is alloyed with Ag, only small amount is available to react with boron. However, this is not the case for Cu cladded wires. Formation of thin  $\text{MgCu}_2$  layer around the superconducting core prevents the further losses of Mg (Matienez et al, 2002; Zhou et al., 2002). The Mg rate in the end product is also affected by the core sheath interface surface versus the core volume, temperature of annealing and annealing time. At the end of the experiment made by Ag, Cu and Fe sheets, it is revealed that as the heat treatment temperature is increased from 600 to 700 °C, the critical current density of Ag sheeted tapes remains constant. Above 700 °C up to 800 °C it decreases continuously and at 800 °C  $J_c$  vanishes. For Cu sheeted tape,  $J_c$  increases and the best  $J_c$  values achieved around 800 °C, than  $J_c$  begin to decrease and vanish at 850 °C. Fe cladding gives the same  $J_c$  values between 600 and 700 °C. Above 800 °C in contrast to the Cu-sheathed tapes the  $J_c$  value continues to increase. In the temperature range between 600-800 °C although the most pure  $\text{MgB}_2$  phase is formed in the Fe sheated tapes, the  $J_c$  values are higher in the Cu-sheathed ones. Even both a larger amount of impurity phases makes the effective area of the superconducting core cross-section smaller and more percolating supercurrent flow which may cause a decrease in  $J_c$  values, in the given temperature range increase of  $J_c$  value may be a result of vortex

pinning enhancement of impurity phases (Zhou et al., 2002). Above the given temperature range the critical current densities in Fe sheathed wires continuous to increase while that for Cu sheathed ones decreases because of reactions (Zhou et al., 2002). Short sintering causes less reaction between sheath and MgB<sub>2</sub> and can increase the J<sub>c</sub> values of Cu and Ag sheathed wires. On the other hand, still Fe gives better results (Soltaian et al., 2002). When Fe used between Cu clad and MgB<sub>2</sub> as buffer layer, it prevents the reaction of Cu with the core at higher temperatures. Even after sintering about 900 °C, well-defined Cu and Fe clad was distinguishable from the core. In studies conducted with stainless steel and Cu-Ni tubes with Cu-10 wt % Ni without heat treatment result in better J<sub>c</sub> values for stainless steel cladding due to the higher packing density of MgB<sub>2</sub>.

Mechanical deformation from round wire to flat tape sample under 620 °C also has different effects on the J<sub>c</sub> when Ag, Cu and Fe cladding is used. Best results are obtained with Cu cladding is a sign of that with Fe cladding optimal density of core achieved by small deformations. In addition hardness of Fe prevents huge deformation, since it breaks. Ag sheathing also shows a poor performance in this case (Zhou et al., 2002)

Filling factor is another important factor. Wires and tapes fabricated by lower filling factor are expected to show higher J<sub>c</sub> values (Suo et al., 2002; Grasso et al., 2001) For example it is shown that a decrease in this factor leads better J<sub>c</sub> values (Grasso et al., 2001). Further enhancement of both critical field and irreversibility field is possible by a reduction in grain sizes. When the grain size is large tight packing of grains become difficult compared to the MgB<sub>2</sub> tapes and wires obtained by using fine powder. Also the grain size may affect the pinning properties. (Beneduce et al., 2002; Zhoa et al., 2002a). However, the upper critical field remained unchanged (Beneduce et al, 2002). On the other hand, the procedure used for obtained finer grains strongly affects the results. In this process, the impurities can be added to the structure or oxygen absorption can occur by grains because of having large effective surface area of grains compared to their volumes. The resulting J<sub>c</sub> values may decrease or increase (Suo et al., 2002; Zhoa et al., 2002a). Moreover the grain size can also be decrease by some dopant like Zr and Ti addition of this material decrease the growth rate of MgB<sub>2</sub> grain (Zhoa et al., 2002a). In MgB<sub>2</sub>/Fe tapes, mono-filamentary ones give better J<sub>c</sub> values than multi-filamentary ones. This may result from intermediate annealing applied in multi-filamentary tape fabrication (Suo et al., 2002) and poor grain connectivity.

In practice, the power transmission cables must preserve their superconducting properties when subject to large strain and stress. It is shown that MgB<sub>2</sub>/stainless steel conductors have a large possibility to be used in practice. They have critical strain almost doubling that of Bi-2223/Ag tape. Here critical strain represents the strain where rapid decrease of critical current density ( $J_c$ ) occurs (Kitaguchi et al., 2001).

To further improve the  $J_c$  in the wires and tapes, the grain linkage and presence of pinning centers are other points, which need to be taking into care. Fabrication of the core/sheath composites is a way to increase linkage between the grains. In this method, PIT technique in the previously mentioned studies employed by addition of metal powders to MgB<sub>2</sub> to form the core of tape or wire. After several attempts done with Ni, Cu, Ag, In and Sn (Tachikawa et al., 2002a) it is revealed that presence of soft metals with low melting points such as Tn and Sn enhance the critical current when compared with the samples produced without any addition of them. Also Ag addition leads slight positive effect. On the other hand, the addition of Cu results a significant decrease in  $J_c$  of the tapes. Similarly Ni also decreases  $J_c$  but this result is interpreted as depending upon the decrease in the effective path.

As previously mentioned grain size is an important parameter. In addition to drawing, rolling and high pressure applications, addition of some impurities in synthesis stage of MgB<sub>2</sub> like Zr and Ti at ambient pressure also lead a reduction in grain size (Zhoa et al., 2002a). Zr and Ti prevent the large grain growths and form a very thin layer of TiB<sub>2</sub> and ZrB<sub>2</sub> around the grains. While without addition of these materials, the large grain sizes lead to a decrease in effective surface area which may be important pinning centers and existent impurities between the grains may reduce the grain connectivity. After doping with Zr and Ti, the resultant small grain sizes of MgB<sub>2</sub> and similarity between the crystal structures of MgB<sub>2</sub> and TiB<sub>2</sub> or ZrB<sub>2</sub> leads extremely tight packing by preventing formation of phases with different crystal structure like MgB<sub>4</sub> (Zhoa et al., 2002a).

Tight packing of grains and factor of Ti in increasing pinning effects also anticipated by another report with the samples prepared under ambient pressure with Ti doping highly dense and good performed bulk materials under various magnetic strength has achieved (Zhoa et al., 2001).

The samples obtained with these techniques denser than that synthesis under several GPa (Zhoa et al., 2002). In addition, Ti doping increases the  $J_c$  values of the samples

with respect to pure ones. On the other, hand it degrades faster by the increasing applied field above the 10 Oe (Zhoa et al., 2001).

In view of obtaining higher upper critical fields than pure substance, improvement of such characteristics through structural or microstructural modifications becomes important. In this manner, the substitutions and doping of MgB<sub>2</sub> with other materials also form research area which should be take in to consideration and may be employed to obtain well tailored MgB<sub>2</sub> superconductors for different purposes. Most of the experimental studies performed to observe the effects of different substitutions and dopants are experienced by fabrication of pellets.

#### **2.4 Effect of Substitutions on Superconducting Properties of MgB<sub>2</sub>**

Addition of other materials not always ends with the substitutions to MgB<sub>2</sub> structure. The significant substitutions only have been achieved for a few substances and after some optimum amount phase transitions and strong degradation of superconducting properties observed. The solubility limits of various substances have been reported in the literature and in these studies there is no case other than one exception where chemical substitution has increased the T<sub>c</sub> above the value given for pure MgB<sub>2</sub> (Hinks et al. 2002; Moritomo and Xu, 2001). On the other hand, in a theoretical study effects of C and Cu substitutions in MgB<sub>2</sub> are searched and it is estimated that replacement of Mg by Cu and low C substitution in the B sheathes can increase the T<sub>c</sub> of MgB<sub>2</sub> (Mehl et al., 2001). In a series of study made with Mg<sub>1-x</sub>Li<sub>x</sub>B<sub>2</sub>, Mg<sub>1-x</sub>Cu<sub>x</sub>B<sub>2</sub>, Mg<sub>0.95</sub>Cu<sub>0.05</sub>B<sub>2-x</sub>C<sub>x</sub> and Mg<sub>0.80</sub>Li<sub>0.20</sub>B<sub>2-x</sub>C<sub>x</sub> indicates that T<sub>c</sub> remains almost constant with increase in hole concentration and decrease with increasing electron concentration. If general formula of this compound is stated as Mg<sub>1-y</sub>M<sub>y</sub>B<sub>2-x</sub>C<sub>x</sub> where M=Li, Cu, this structure is electron doped in the case of x-y>0 and x-y<0 for hole doped case (Balaselvi et al., 2002).

While the studies are in an agreement for the contraction in parameter *a* by substitution of MgB<sub>2</sub> by Li, there are contradictory results claiming decreasing (Li et al., 2001) and constant values (Zha et al., 2001) for parameter *c*. Na substitution leads and increases both *a* and *c* values, on the other hand higher concentration decreases these parameters. T<sub>c</sub> slightly decreases with Li substitutions (≈0.6 K) when x exceeds 0.5 in Mg<sub>1-x</sub>Li<sub>x</sub>B<sub>2</sub> the material losses superconducting properties (Cimberle et al., 2001; Li et al., 2001; Zha et al., 2001). Presence of small amount of Li enhances the J<sub>c</sub>

(Cimberle et al., 2001). For Na substitutions there is no apparent change of  $T_c$  (Zha et al., 2001).

A significant suppression occurs in  $T_c$  values as a result of Mn substitutions to the  $MgB_2$ . Al also decreases  $T_c$  but less than Mn for small doping levels. For example while at  $x=0.05$  the  $Mg_{1-x}Mn_xB_2$  structure take a  $T_c$  value around 30 K (Xu et al., 2001) in the same range of  $x$  for Al substitution  $T_c$  onset is obtained around 37.2 K (Cimberle et al., 2001; Slusky et al., 2001). Presence of small amount of Al can also enhance  $J_c$  (Cimberle et al., 2001). Change in  $T_c$  interpreted as result of reduction in density of states at Fermi level  $N(E_F)$  (Kotegawal et al., 2002). Increasing Mn and Al substitutions leads further decrease in the values (Xu et al., 2001; Dong et al., 2001). Moreover with more Al addition phase transitions have been observed at the 17% and 75% doping levels. 50% doping leads a  $MgAlB_4$  structure with a transition temperature about 12 K (Dong et al., 2001). Solubility of substituents is a factor need to be considered. As in the case of Al dopants beyond some concentration materials can form other structures in place of substituting in structure of  $MgB_2$ . Doping  $MgB_2$  with Cu is a difficult task. The reason of this is the high affinity of Mg and Cu to form cubic inter metallic compounds with a Cu/Mg ratio ranging from 2/3 to 3. As a result of this attempts to synthesize of solid solutions  $Mg_{1-x}Cu_xB_2$  with Cu were not successful and these solids solutions attained by use of  $CuB_{24}$ . Even with this way substitution with ranging from  $x=0.003$  to 0.03 become possible. In this range increase in the substituent concentration results with a nearly 0.5 K degradation in  $T_c$  at  $x=0.03$  (Tampieri et al., 2002). Almost 0.4 K decrease occur in the  $T_c$  values of Si substituted samples and one of the steepest transition occur with Si substitutions with a  $\Delta T=0.7$  K (Cimberle et al., 2001). Hysteresis loops measured at low temperature indicate an improvement of the critical current density about a factor 3 with the Si doping. Zn also led only slight changes in  $T_c$  value in negative direction (Xu et al., 2001). Although it is not confirmed there is only one study asserting that Zn substitution with  $x=0.003$  result in a  $T_c$  increase around 0.2 K and decreases in the other studies explained by presence of excess Zn over the optimum dose around  $x=0.004$  (Moritomo and Xu, 2001). Superconducting state of  $MgB_2$  is amenable to the spin impurity (Xu et al., 2001).

It was suggested that Ta powder addition to the starting composition of B and Mg leads an increases of critical current densities. The presence of Ta foil around the tablet samples also an enhancing factor of  $J_c$  (Priyha et al., 2002).

As a result of mixing of 5 mole % each of fine particles of Fe, Mo, Cu, Ag, Ti and Y with as received MgB<sub>2</sub> powders in clad metal and heat treatment around 900 °C it was showed that presence of this particles have only little effect on the T<sub>c</sub> of MgB<sub>2</sub>. Due to the mutual solubility of Y with Mg and reactivity with B, some broadening of transition was observed. On the other hand J<sub>c</sub> studies revealed that J<sub>c</sub> could be significantly reduced. While Fe addition appeared to be least damaging Cu addition can significantly reduce that value on the 2-3 orders of magnitude. The addition of other metals takes values between these, two materials. This behavior can be attributed to the formation of reacted layers around the grain boundaries. While Ag, Y and Ti can react with both Mg and B, Cu can react with Mg and Fe and Mo react with boron. The presence of such layer can cause weak link problems (Jin et al., 2001).

It is theoretically predicted that Be substitution for B is unfavorable (Mehl et al., 2001). The solubility of carbon in boron is probably less than 2.5 % and the presence of carbon is detrimental to the superconductive properties of MgB<sub>2</sub> samples (Paranthaman et al., 2001). Experiment with MgB<sub>1.8</sub>C<sub>0.2</sub> pellets leads two distinct onset temperatures one at 41 K the other is at 37 K and compared with MgB<sub>2</sub> transition width of this samples are very broad. Also with this composition single phase of material obtained with smaller B-B bond and only small amount of MgO impurities (Ahn and Choi, 2001).

There are only a few studies directly related with effect of excess Mg and Mg/MgB<sub>2</sub> composite fabrication. One of them is a microstructural study of in-situ formed MgB<sub>2</sub> phases in a Mg alloy matrix composites reinforced with SiC whiskers and B<sub>4</sub>C particles without any attribution to superconducting and mechanical properties of the resultant products (Chen et al., 2002). Mg/MgB<sub>2</sub> composites produced by liquid infiltration technique, in which pure Mg infiltrated in to the tapped commercial MgB<sub>2</sub> powder perform, found to have high density and transition around 38K with much larger transition than pure samples MgB<sub>2</sub> prepared by this group. In another method followed by same group had showed the possible synthesis of MgB<sub>2</sub> by the liquid infiltration of B perform with Mg possessing a transition around 37 K. Further annealing of this samples results a superconducting transition around 39 K with very brittle structure and pure mechanical properties (Dunand et al., 2001). In another report effect of unreacted Mg in MgB<sub>2</sub> was given as broadening of transition temperature and increasing the RRR ( $\rho(300\text{ K})/\rho(40\text{ K})$ ) values (Jung et al., 2002b). Despite these results it was also claimed

that small amount of excess Mg slightly increases  $T_c$  with respect to that of commercially available  $MgB_2$  (Jin et al, 2001).

## 2.5 Effect of Pressure

The response of transition of  $MgB_2$  is negative to the highest pressure studied in literature. An interesting point in the studies is that samples with lower  $T_c$  at zero pressure have much steeper  $T_c(P)$  dependence than the samples with higher  $T_c$ . In addition to these, the lattice parameter along the c axis decreases faster with pressure than along the a-axis. This implies that the out of plane Mg-B bonds are much weaker than in plane Mg-Mg bonds (Buzea and Yamashita, 2001).

Regardless of the negative effect on the  $T_c$ , production of  $MgB_2$  under high pressure seems to be very promising because of the resultant highly dense structures. Samples with a 95-97 % of the theoretical density were achieved with both pressure and heat treatment (Priksa et al., 2002). Since the grain connection in denser structures are more than porous ones pressure affect the  $J_c$  in a positive manner. Even the hot isostatically pressing of commercially available  $MgB_2$  around 950 °C and 100 MPa leads 2 K decrease in the  $T_c$  100% dense samples with superconducting homogeneity are obtained (Shields et al., 2002). The density of samples was measured as  $2.63 \pm 0.02 \text{ g.cm}^{-3}$  which is very close to the theoretical density of  $2.625 \text{ g.cm}^{-3}$  (Indrakanti et al., 2001).

Although the application of pressure increase grain connectivity, decrease the decomposition during the sintering and aid to obtain denser structures, practical use in large dimensions are limited as previously mentioned. However it is possible to attain large bulk manufactures in an inexpensive way with liquid infiltration technique, without need of high-pressure apparatus (Giunchi et al., 2002).

In addition, since the stress introduced among the grain boundaries do not relieve, stress effect could be greatly amplified in the samples made at a high pressure (Ribeiro et al., 2002, Hinks et al., 2002).

## 2.6 Effect of Sintering

A large increase of  $J_c$  is observed in many studies of with annealing of samples. If annealing is performed in the presence of the other materials like in PIT or in fabrication of composites, this enhancing factor depends strongly on the melting temperature and reactivity of these materials with the  $MgB_2$ .  $J_c$  can increase with

increasing temperature for a while and after some temperature like in the case of Cu (Zhou et al., 2002) and stainless steel (Matsumoto et al., 2002) sheathed wire and tapes it tend to decrease. In addition, the synthesis of  $\text{MgB}_2$  in contact with BN results in similar picture of the  $J_c$  values around 950 °C (Prikha et al., 2002). If the materials are not reactive as in the case of Fe increasing trend of  $J_c$  also valid for higher temperature needed to attain a well behaving  $\text{MgB}_2$  (Zhou et al., 2002; Matsumoto et al., 2002).

The improvements in the  $J_c$  values mainly depend on the linkage of  $\text{MgB}_2$  grains. In Fig. 2.6, SEM pictures demonstrates effect of increasing sintering temperatures on the samples prepared with same composition and with same pressure. It is apparent that higher sintering temperature results with better grain connectivity and less porous structures.

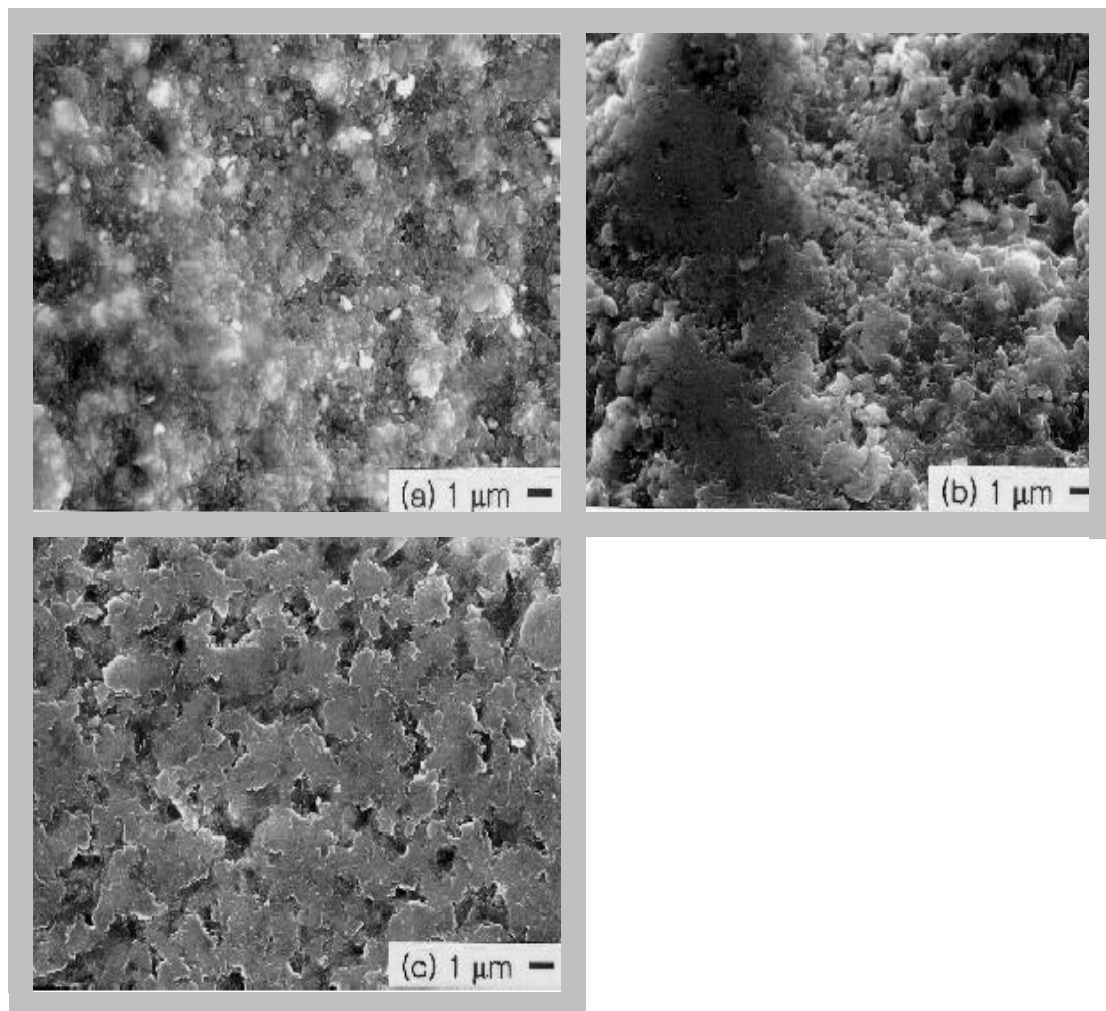


Figure 2.6 SEM images reflecting effect of sintering (Jung et al., 2001)

When high temperatures are attained, loss of Mg in vapor form is needed to take in to care especially when in in-situ production of MgB<sub>2</sub> will be employed. While the weight loss during the sintering of ribbons at 900 °C in argon atmosphere was only about 0.8% after same sintering condition around 31% lost of weight was observed. The weight loosed in the pellets almost equivalent to 60% loss of Mg (Jin et al., 2001). With such a heat treatment of pellets no more benefit of sintering is observed because of having highly porous structure (Jin et al., 2001; Slusky et al., 2001).

As in the case of pressure applications the lattice parameter along the c axis decreases faster with temperature than along the a-axis (Buzea and Yamashita, 2001).

Figure 2.6 illustrates the effect of sintering on MgB<sub>2</sub> made under 3 GPa (Jung et al., 2001). The scale bars are 1 μm in length. The sintering temperatures were a) 20 °C, b) 500 °C, and c) 950 °C. The sample without actual heating, (a), shows well-separated grains with spacious voids. As the sintering temperature is increased, the connectivity of each grain increases and porosity decreases rapidly.

## CHAPTER 3

### EXPERIMENTAL METHODS

#### 3.1 Sample Preparation

Commercially available 325 mesh powders of  $\text{MgB}_2$  obtained from Alfa Aesar and 270 mesh powders (powders 38-53 mic. in diameter) of Mg obtained with a steel file followed by sifting through Retsch D-42759 stainless steel sieves are mixed homogeneously. Since the purity of constituents in Mg/ $\text{MgB}_2$  MMCs are important in the superconducting properties, at the sifting stages Mg and sieves were very carefully handled to prevent contaminations of Mg. For samples, mixtures of 3 g of  $\text{MgB}_2$  and Mg powders of 5%, 10%, 15%, 20% weight ratios of the  $\text{MgB}_2$  are prepared for pressing in the form of pellets.

In each time one of these mixtures is inserted in a heat-treated steel die as depicted in the Fig. 3.1. The die has inner radius of 7.81 mm and outer radius of 60 mm. After that the die is placed in heating resistors and Carver 3925 laboratory hydraulic pressure equipment. This equipment has maximum 12-ton pressure capacity. With the aid of these equipments, hot uniaxial pressing carried out with application of 0.5 GPa pressure and heat treatment of about 400 and 500 °C for 2 hours. After pellet formation was completed, the sample was removed from die by use of a hollow cylinder and some pressure as shown in Fig. 3.2. During this process temperature control is made by Omega thermocouple system and a variac. As a control group pure  $\text{MgB}_2$  pellets of Alfa Aesar powders are also prepared for each sintering temperature.

At the end of these stages, we prepared totally ten samples, 5 for each sintering temperature. The final samples are tablets about 0.9 mm in thick and 15.62 mm in diameter. To measure resistivity, samples are sliced in to bar like pieces. The number of samples, their empirical and theoretical densities and their mutual ratios are given in Table 3.1.

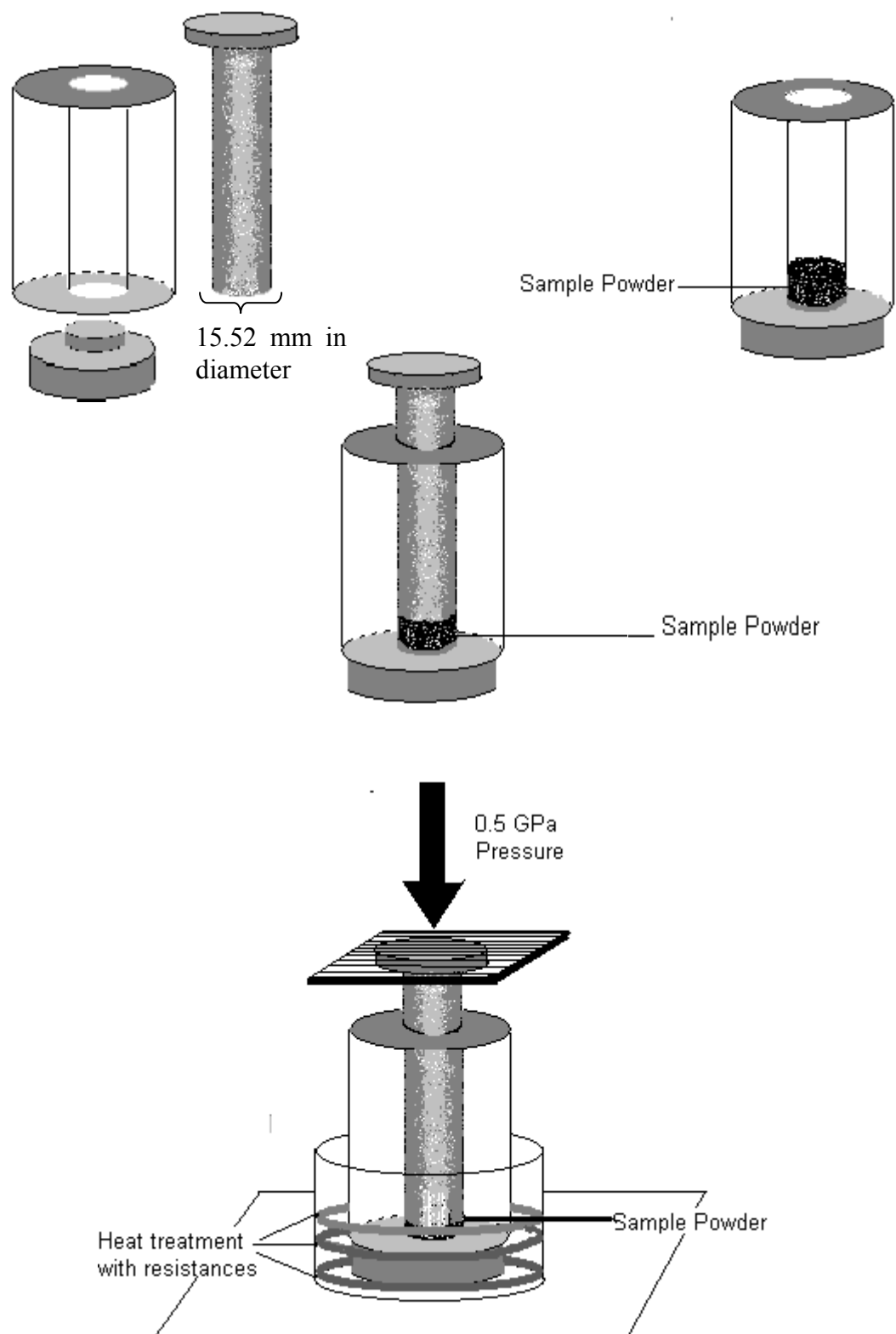


Figure 3.1 Fabrication of Pellets

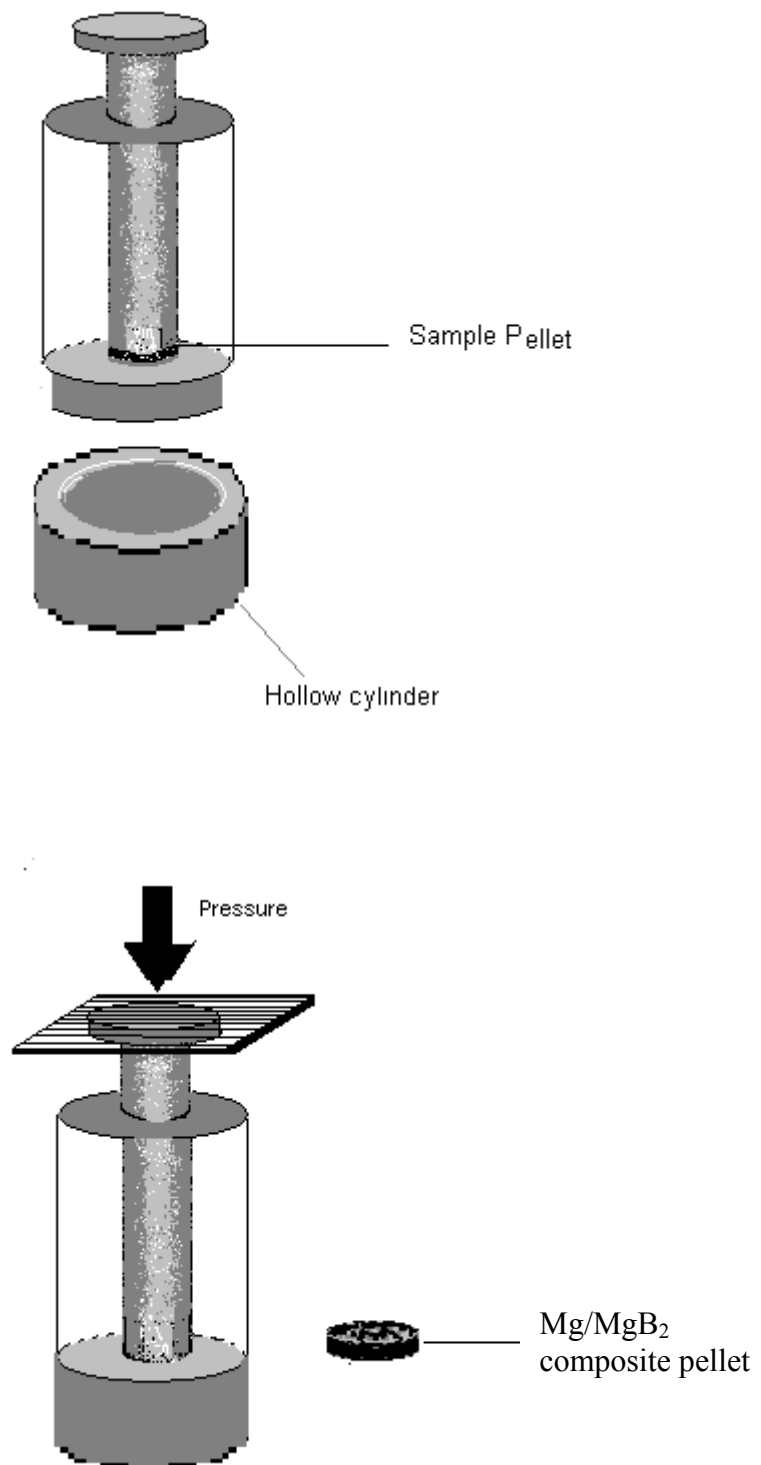


Figure 3.2 Fabrication of Pellets

Sample Number:	Mg/MgB <sub>2</sub> Weight Ratio	Temperature of Applied Heat Treatment	Density (x10 <sup>3</sup> kg/m <sup>3</sup> )	Theoretical densities (x10 <sup>3</sup> kg/m <sup>3</sup> )	Empirical Density /Theoretical density
400	pure	400 °C	1.63	2.625	0.620
405	5%	400 °C	1.7	2.583	0.658
410	10%	400 °C	1.8	2.544	0.707
415	15%	400 °C	1.82	2.509	0.725
420	20%	400 °C	1.92	2.477	0.775
500	pure	500 °C	1.69	2.625	0.644
505	5%	500 °C	1.89	2.583	0.731
510	10%	500 °C	1.98	2.544	0.778
515	15%	500 °C	2.00	2.509	0.797
520	20%	500 °C	2.12	2.477	0.855

Table 3.1 Sample numbering, Mg concentrations, annealing temperatures and densities.

### 3.2 Measurements

At critical temperature, the transition of a material from normal state to superconducting state by acquiring perfect diamagnetism and zero electrical resistance brings about two methods for the determination of critical temperature, namely resistance and magnetic susceptibility measurements. Even the both method serve for this purpose, in this study we had used resistive method. To make measurements,

unpolished Mg/MgB<sub>2</sub> composites, fabricated under a pressure of 0.5 GPa were cut in to pieces by diamond-saw with appropriate dimensions. We could not polish the samples because of surface fracturing. The samples were prepared by use of four-point probe technique (Fig. 3.3) to place in cryosystem given in Fig. 3.4.

### 3.2.1 Four Point Probe Method

Four-point probe method is one of the most widespread methods in the T<sub>c</sub> determination. In this study, to make measurement, copper wires with 0.1 mm in diameter are connected to sample at four points by use of a silver paint as demonstrated in Fig. 3.3. Two of the four contacts on the samples belong to current carrying cables (1 and 4) and the other are attached to the two voltage measuring cables (2 and 3). The reason for the choice of this technique rather than use of two probes is that in the latter one the contact and spreading resistance cannot be separated from measured resistance. On the other hand in the four-point probe method when the current applied from the outer two wires, the voltage measured from the inner probes is not influenced by the resistance at the contact and wires. The inner probes only measure the voltage of the material and do not transmit electrical current. Since applied current and voltage across the inner probes are known, one can easily determine the resistance of the sample from the Ohm's law. Thermal conductance (between cold head and sample) and stability enhanced by use of vacuum grease.

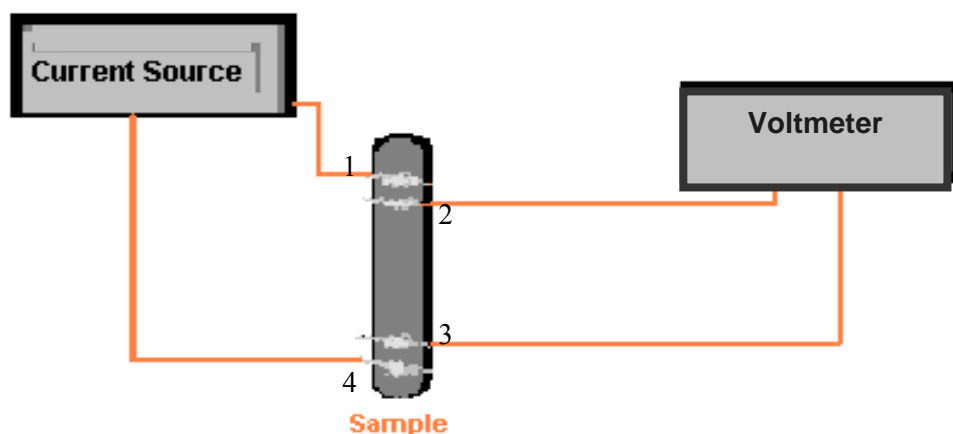


Figure 3.3 Four Point Probe Method

### 3.2.2 DC Resistance Measurements

After the preparation of the samples with four-point probe method, we determine the change in the resistance of them with the utilization of computer controlled cryo system of which schematic representation is given in Fig. 3.4. The system provides us a sensitive measurement of resistivity from room temperature down to 12 K.

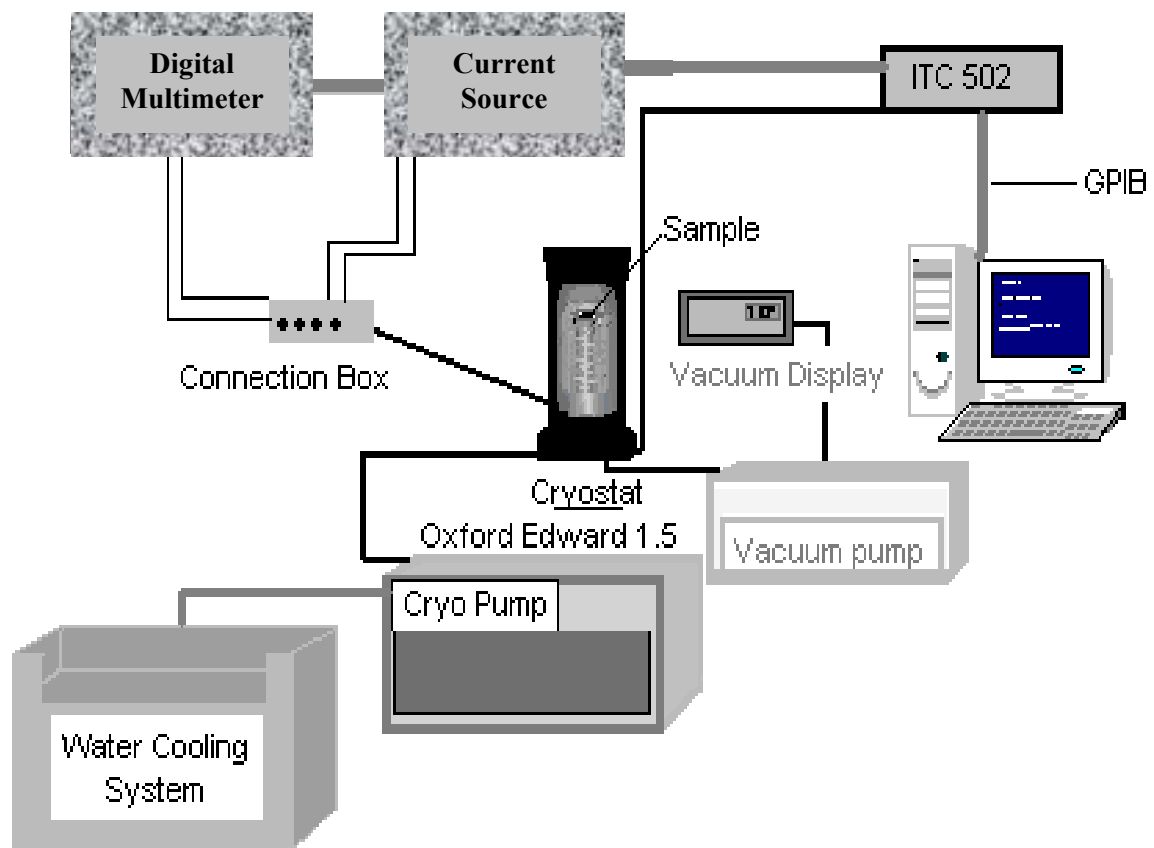


Figure 3.4 The Cryo System

The system consist of an Oxford Edward Cryostat 1.5 (a closed system helium cryostat), Coolstar Cold Head model 2/9, Keithley 220 current source, Keithley 2000 Digital Multimeter, a water source to cool the Cryodrive, Leybold Trivac Vacuum Pump, ITC 5002 temperature controller, Termovac Sensor with tungsten filament for vacuum measurement, GPIB connectors and IEEE 488.2 interface card for the connection to the computer. The data taken from the system had been processed by an Object Bench program and simultaneously converted to R versus T graph on the screen

as the experiment goes on. To get rid of offset effects in the system, the arithmetic average of absolute value of voltages obtained by changing the polarity of the applied current were taken by the program. Temperature measurements were performed by use of the Rd-Iron Temperature Sensor. ITC 502 Temperature Controller unit with P-I-D control parameters are used to control temperature and Helium flow rates. The data are taken after the achievement of a vacuum medium in the cold head on the order of  $10^{-3}$  Torr. For each samples the resistance measurements were done for 1 mA, 5 mA, 10 mA, 50 mA and 100 mA.

## CHAPTER 4

### RESULTS AND DISCUSSIONS

To determine superconducting properties of our MgB<sub>2</sub>/Mg metal matrix composites, we applied resistivity-temperature measurements, XRD, SEM and EDX methods. In this part, I will mainly mention about the results of these measurements.

To clarify the composition of samples, XRD results are demonstrated in Fig. 4.1 and Fig. 4.2 for 400 and 500 °C heat-treated samples, respectively. As the initial concentration of Mg increases, Mg peaks become clearer. Even no other phases than MgB<sub>2</sub> and Mg are observed in these peaks, examination of XRD results with search match indicates the possible presence of MgB<sub>4</sub>, MgB<sub>6</sub> and MgO. Although there are no evident peaks, other impurities found in the initial constituents can exist in these final products in very small amounts. The presence or absence of secondary phases was also examined with EDX. EDX analysis does not lead certain results for the presence of secondary phases, i.e. existence of Mg, B with a weight ratio that suits the MgB<sub>6</sub> stoichiometry not always indicate the presence of MgB<sub>6</sub>. In such circumstance, one not able to state the presence of MgB<sub>6</sub> by only relying on the EDX results which can refer the any combination of the Mg, B, MgB<sub>2</sub>, MgB<sub>4</sub> and MgB<sub>6</sub>. EDX results based on the relative atomic weights and may be misleading especially for light substances or for substances with close atomic weights. On the other hand, the search match results of XRD also confirm the results. Presence of MgO particles may enhance the superconducting properties by acting as pinning center by preventing motion of vortices. On the other hand, the presence of MgB<sub>4</sub> is undesirable, since it is generally situated around grain boundaries with large mismatch in the crystal structures. As a result, the presence of MgB<sub>4</sub> causes a loose connection between grain boundaries. Except MgO, the secondary structures are observed in all of our samples and they probably come from commercial powder. MgO concentration might be increased during the heat treatment. Presence of these phases was also detected in the XRD analysis of a similar study on hot isostatically pressed MgB<sub>2</sub> pellets of the same commercially available MgB<sub>2</sub> powders around 900 °C (Shields et al., 2002). Since our temperature range is relatively low for the formation of MgB<sub>4</sub> and MgB<sub>6</sub>, and presence of excess Mg prevents the formation of these phases, we do not expect an increase in the concentration of these materials in the samples after the heat treatment. A heat

treatment around 900 °C for pellets leads an enormous weight loss due to the evaporation of Mg (Jin et al., 2001). In our case the temperature that we attained was far from the evaporation point of Mg and enough to soften it under such a pressure. Thus we have not anticipated and observed such a loss of Mg. Moreover from the SEM pictures given in Fig. 4.3 it is revealed that with increasing Mg concentration and temperature porosity decreases. Table 3.1 also indicates a similar result, as temperature and Mg concentration increases the ratio of empirical density to theoretical density increases.

According to SEM images, it looks like that while the grain sizes of  $\text{MgB}_2$  is change in the 0.3-5  $\mu\text{m}$  range for 400 °C heat treated samples, that takes values between 0.2 and 5  $\mu\text{m}$  for 500 °C heat treated samples. Even at first glance this impression is gathered from our SEM images, it is hard to state the result with great precision. We have been only able to study unpolished surfaces because of surface contaminations in the polishing process and surface fracturing. The main disadvantages of fracture surface analysis are the presence of many layers on each other with different depths. In such images, observation of actual grain spacing, sizes and distribution of grains and empty spaces is not possible because of the screening by other grains. Grain size refinement generally either observed by drawing and rolling of metal-sheathed tubes (Jin et al., 2001) or addition of some impurities such as Ti and Zr (Zhao et al., 2002). It has been revealed that while short time annealing at 600 °C does not change grain size of  $\text{MgB}_2$  in the SUS316 tapes relative to un-annealed ones, formation of reacted regions about 10  $\mu\text{m}$  size in some areas with better linkage enhance the superconducting properties of  $\text{MgB}_2$  (Matsumoto et. al., 2002). In other report an increase in the annealing temperature from 900 to 1000 °C (with 30 min duration) for Fe sheathed  $\text{MgB}_2$  ribbons fabricated by commercially available  $\text{MgB}_2$  powder resulted in about 2.5 times larger grain size (Jin et al., 2001). In our study, we had used commercial Alfa Aesar powders with 325 mesh size. These sizes match with a grains equals to or less than 44  $\mu\text{m}$  in diameter and very large compared to the 0.2 and 5  $\mu\text{m}$ . If these results are right applied heat and pressure for two hour leaded a grain refinement and result in grain size more than 1000 times smaller than that of initial powders. Such a result seems to conflict with the previously mentioned reports. Grain refinement permits consolidations at lower temperatures and increases grain boundary pinning (Zhao et al., 2002).

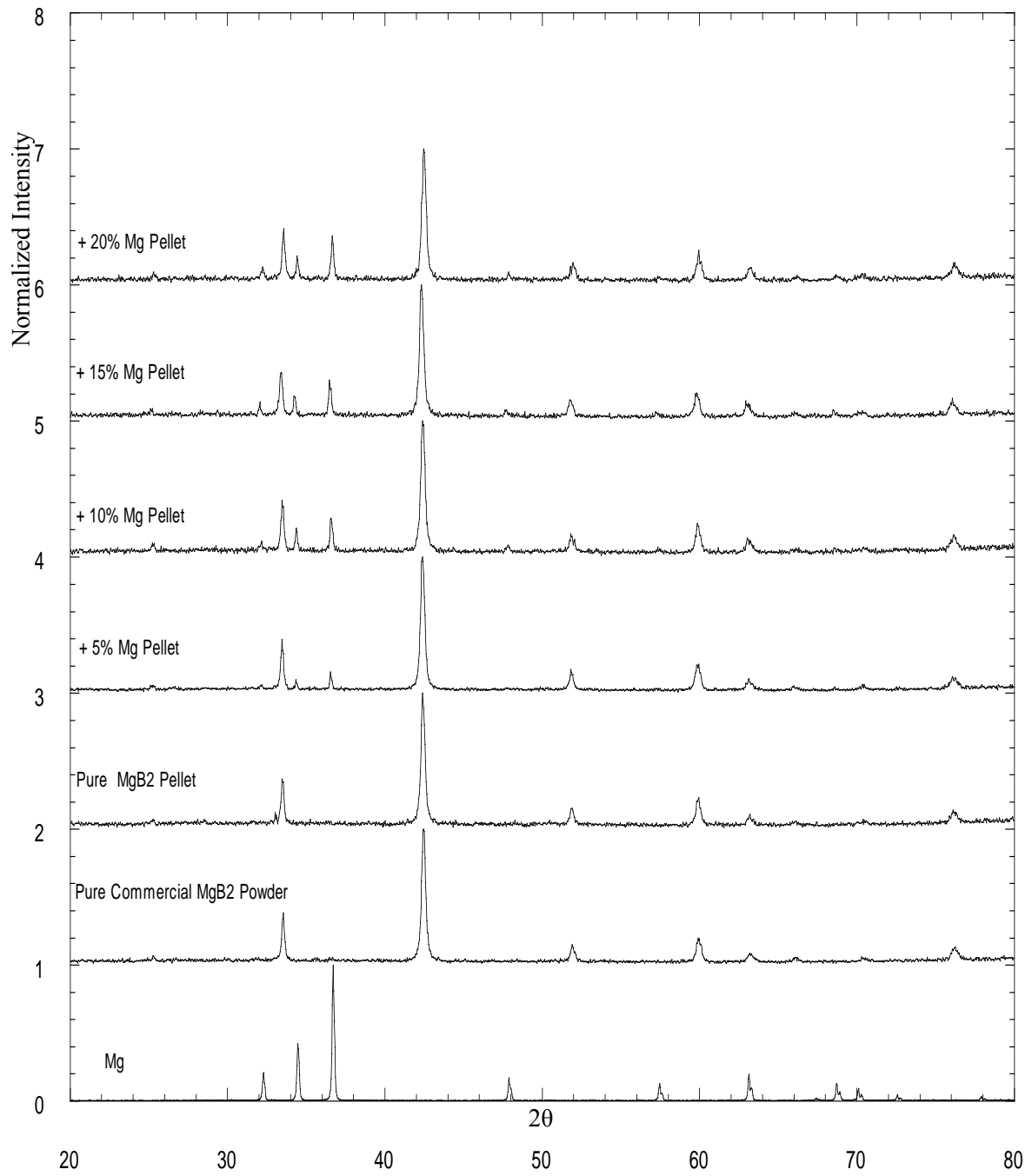


Figure 4.1 XRD Patterns of Samples Prepared at 400 °C

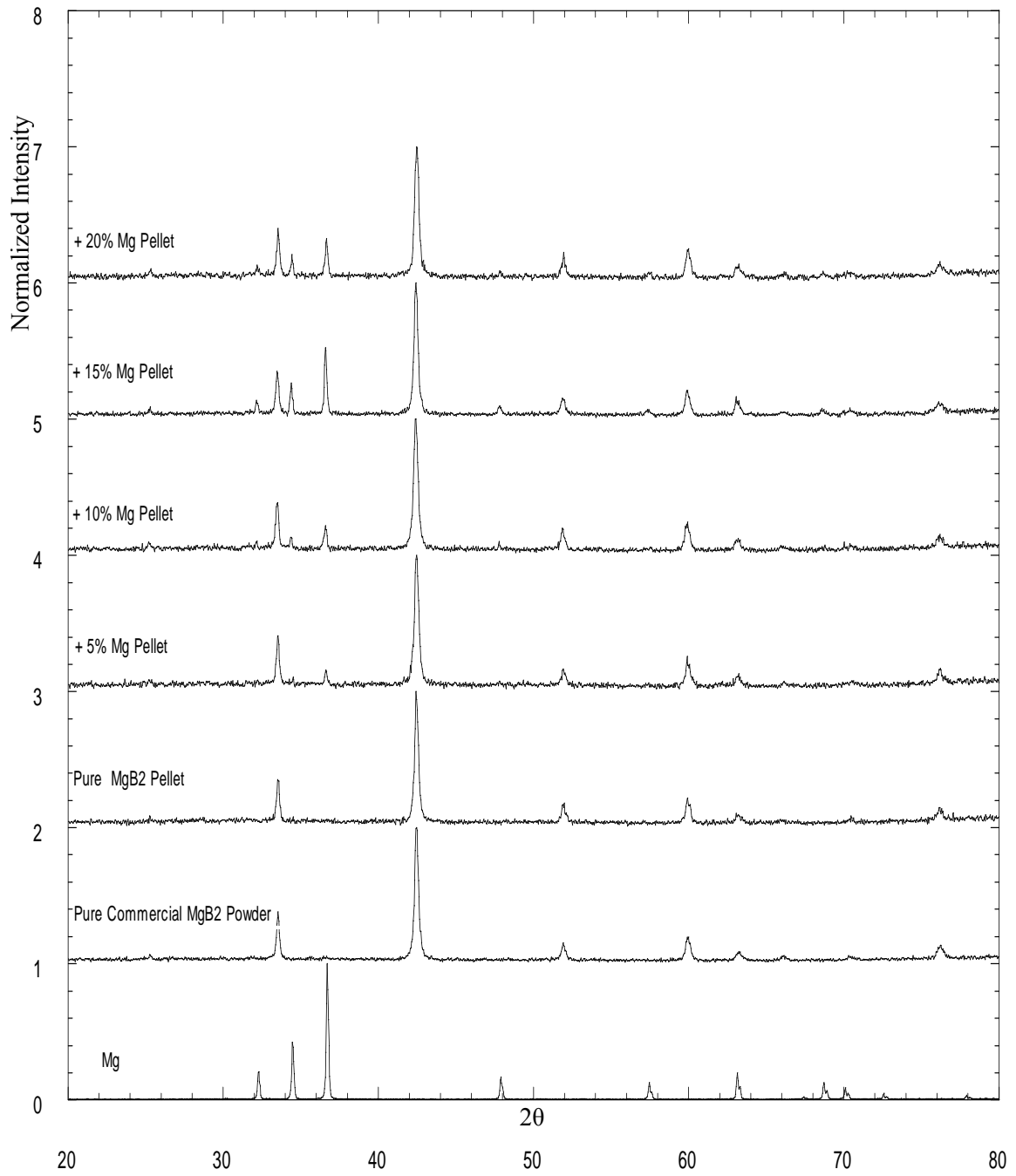


Figure 4.2 XRD Pattern of Samples Prepared at 500 °C

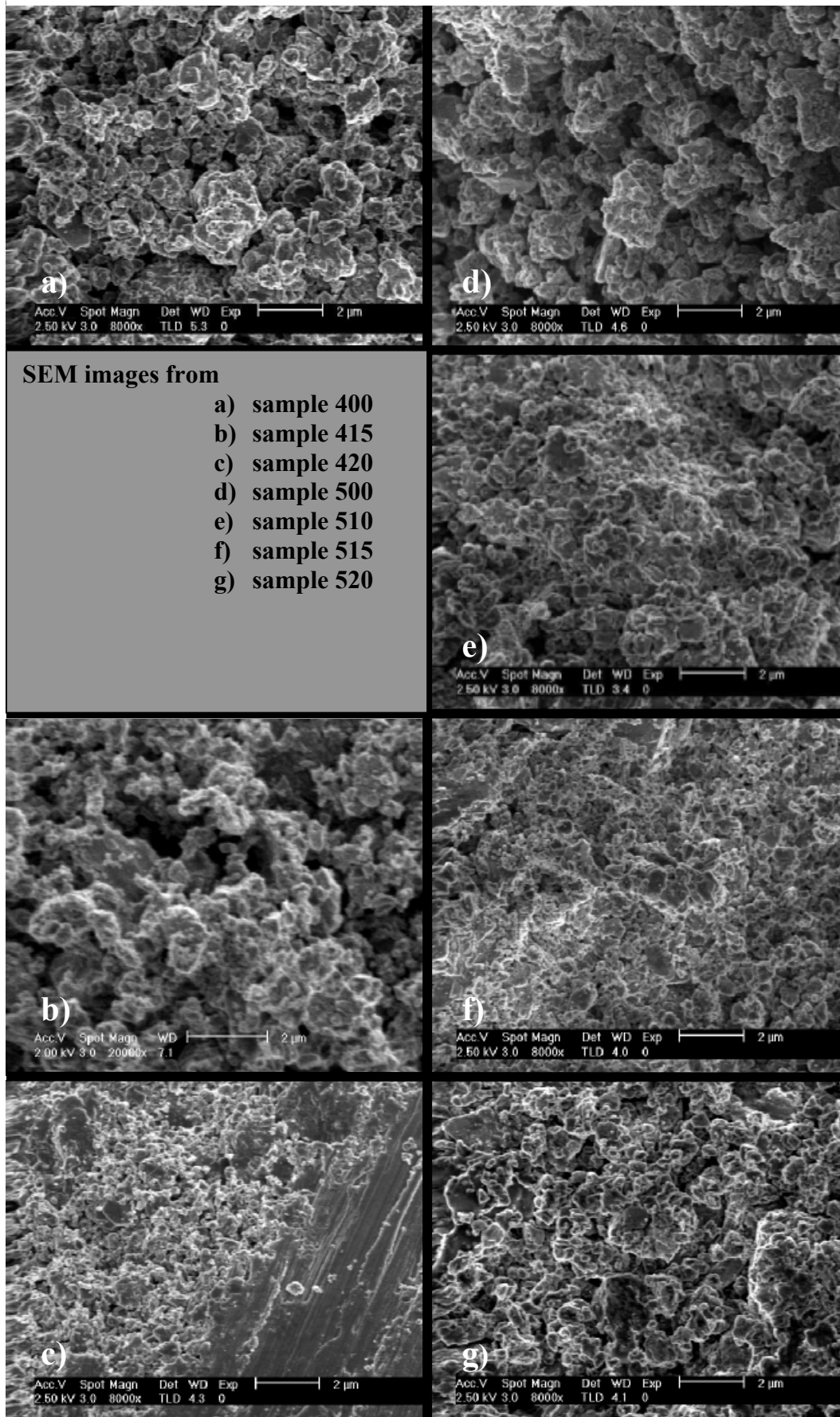


Figure 4.3 SEM images reflecting effect of heat and excess Mg

The SEM images given in Fig. 4.3 illustrate how the heat treatment and increasing Mg concentration affect the grain connectivity and the porosity of the samples. The left side of the figure includes SEM images of the samples prepared at 400 °C and at other side that of samples sintered at 500 °C are given. A 100 °C increase in annealing temperature results in a consolidation of grains as can be clearly viewed from Fig. 4.3(b) and Fig. 4.3(f). In the figure images are placed in an order of increasing Mg concentrations from top to down. As also confirmed by ratio of theoretical density to empirical one the SEM illustrates that increasing Mg concentration and annealing temperature also decreases voids in the samples.

Fig. 4.4 and Fig. 4.5 demonstrate the distribution of Mg grains in the some of our bulk samples. As can be easily observed from the images Mg does not disperse widely and not diffuse to the grain boundaries. Rather it is present in the form of local clusters. Subsequent to the SEM images, some EDX results suggesting the presence of different phases are given.

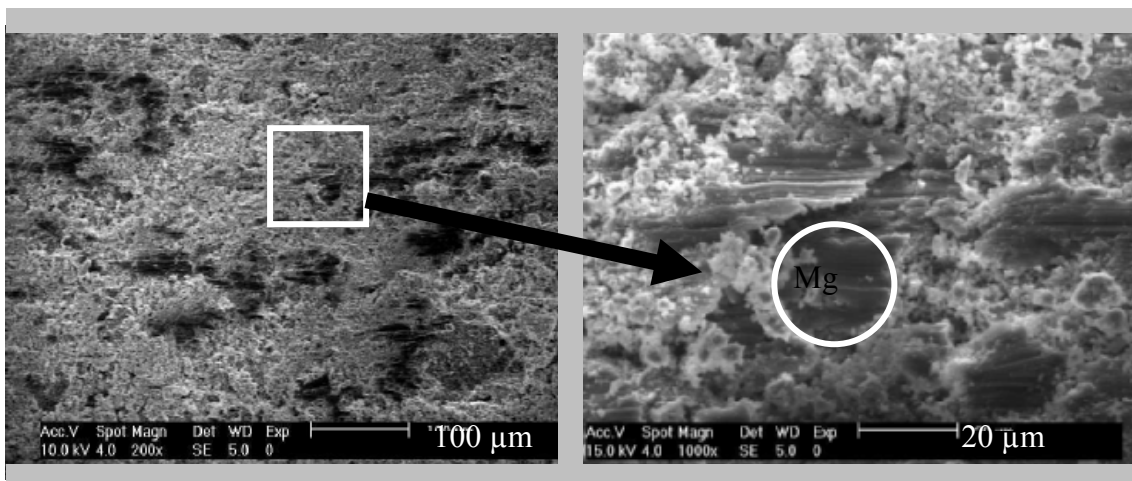


Figure 4.4 SEM images of some Mg rich sides in sample 515.

Fig. 4.4 a) demonstrate a Mg rich side in sample 515. Fig. 4.4 b) is a SEM image of the area enclosed by white rectangle. EDX analysis obtained by focusing in the circle gives us a hint about the existence of unreacted Mg. According to EDX result this part is composed of Mg with a weight ratio of 97.64% and small amount of MgO.

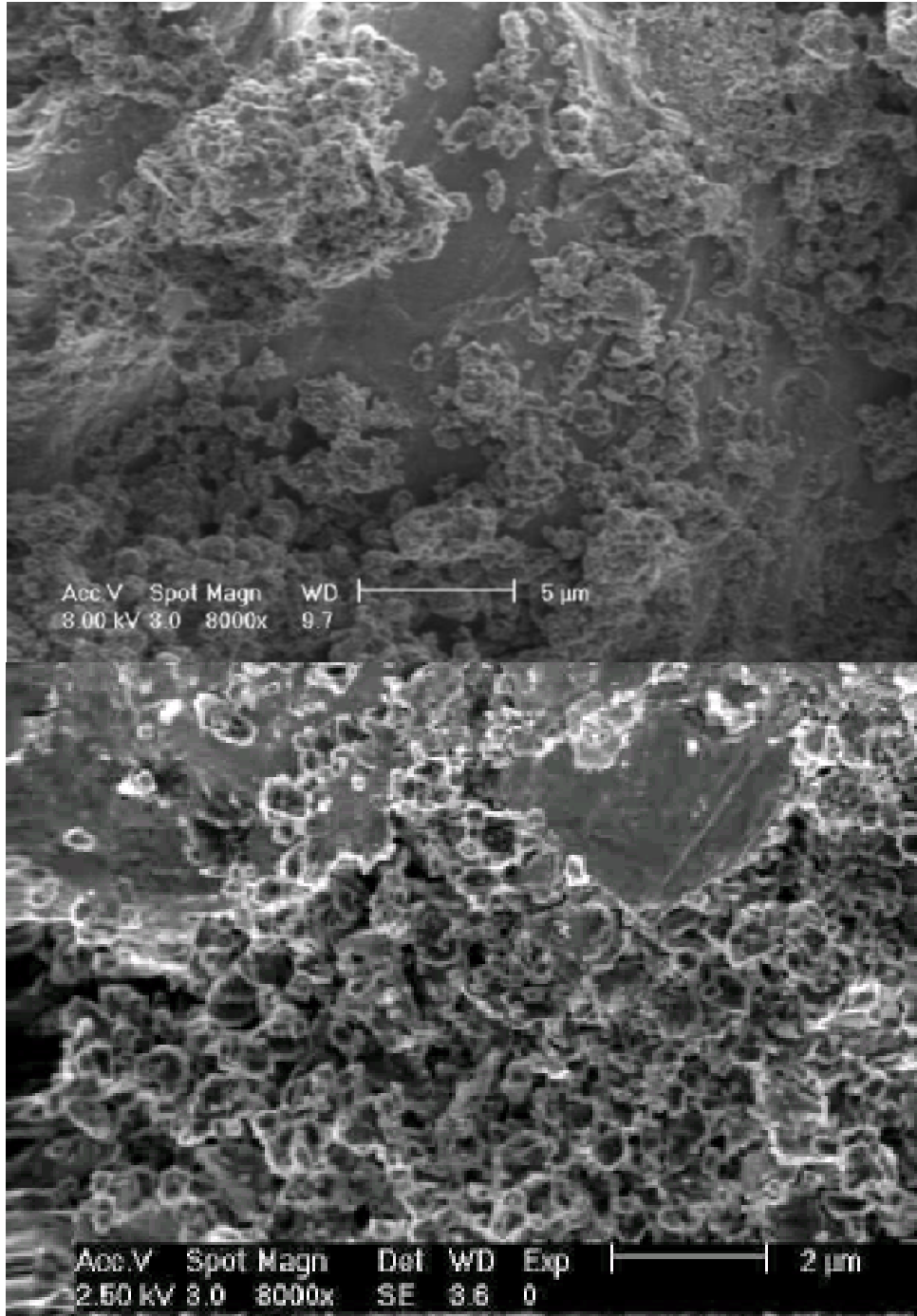


Figure 4.5 Mg Distributions in 405&410

EDX of a local space of sample 500 supposed to be composed of MgB <sub>2</sub> and small amount of MgO.		EDX of a local space of sample 500 supposed to be contain MgB <sub>4</sub> phase.		EDX of a local space of sample 505 rich in B and supposed to be contain secondary phases like Mg B <sub>4</sub> and MgB <sub>6</sub>		EDX of a local space of sample 505 supposed to be rich in unreacted Mg concentration	
Elem	Wt %	Elem	Wt %	Elem	Wt	Elem	Wt
B K	48.19	B K	56.07	B K	73.09	B K	0.00
O K	6.38	O K	8.81	O K	2.57	O K	0.39
MgK	45.43	MgK	35.13	MgK	24.34	MgK	99.61
Total	100.00	Total	100.00	Total	100.00	Total	100.00

Table 4.1 EDX Results of samples illustrating existence of local places of with different compositions

As previously pointed out in the beginning of the Chapter 4 result given in Table 4.1 can only inform us about the presence of elements and their relative amounts. They do not give which combinations of these elements exist. For example in the first column, weight ratio of B to Mg is very close to the stoichiometric ratio in MgB<sub>2</sub> and this region is supposed to be composed of MgB<sub>2</sub> and small amount of MgO. However this is not an absolute proof for the presence of these compounds, other combinations of Mg and B like unreacted B, Mg or MgB<sub>4</sub>, MgB<sub>6</sub> can also be in the region. Considering the initial constituents we can guess that this region mainly consist of MgB<sub>2</sub>.

Similar arguments are also valid for the second and third column, in these parts B is much more than that necessary for the stoichiometry. Commercial MgB<sub>2</sub> powder includes secondary phases (MgB<sub>4</sub>, MgB<sub>6</sub>) in small amounts and these regions are probably includes these phases.

In the fourth column of Table 4.1 the amount of O is not enough to consume all of unreacted Mg to form MgO and obviously EDX analysis of this region denotes existence of unreacted Mg phases in the sample which is necessary for the formation of desired composite structure. Similar analysis was also obtained for the other samples. Since the sintering temperature not high enough to let a reaction of MgB<sub>2</sub> and Mg, this result is not surprising.

## 4.1 Resistivity Results

The critical temperature is one of the most important basic properties of materials that exhibit superconductivity. There are different determination methods of  $T_c$  such as on-set, mid-point, and zero-point ( $T_{c \text{ zero}}$ ). The onset determination is suitable for obtaining the maximum  $T_c$  of the non-homogeneous or multi-phase material. In the industrial use zero-resistance is needed and the onset determination having high resistance shall not be used. Thus zero-point approach is appropriate for industrial use. However determination of  $T_{c \text{ offset}}$  is very hard due to unclear zero-level.  $T_c$  is practically important in the application of superconductors. Thus standardization of determination of  $T_c$  is quite beneficial. The midpoint frequently applied for this aim in  $T_c$  determination. In this thesis, I also use midpoint approach by considering the study published for the sake of standardization (Murase et al., 2001).

In this method, first a tangential line to a part of curve in the normal state region is drawn. The value of temperature at the intersection of the transition curve and a line with 50% height of the tangential line (50% resistance) is determined as  $T_c$ . In addition two temperature values at the intersections of the transition curve and two lines with 10% and 90% heights of the tangential line are denoted by  $T_{c0.1}$  and  $T_{c0.9}$ , respectively and the transition width,  $\Delta T_c$  is defined as  $T_{c0.9} - T_{c0.1}$ .

Simple demonstrations of this technique are given in Fig. 4.6 for samples prepared by 400 °C and with 15% excess Mg. The resistivity curves belong to the 5 mA and 10 mA current applications, respectively. As can be viewed from these two graphs  $T_c$  can/cannot match with the 0.5 on the y-axis.

From figure 4.7 through 4.11 resistivity-temperature graphs of the samples annealed at 400 °C are given for five different currents. The resistivities in the graphs normalized to one at 50 K.  $T_c$ ,  $T_{c \text{ onset}}$  and  $\Delta T_c$  values determined from each curve are listed in tables following the figures. Figure 4.9 and 4.10 illustrate impracticalness of zero point approach in  $T_c$  determination. Superconducting transition is incomplete in 100 mA measurements and  $T_{c \text{ offset}}$  cannot be determined.

A similar analysis for 500 °C heat treated samples is demonstrated between the pages 51 and 55. To observe the effect of increasing Mg concentration on transition, 100 mA resistivity-temperature results of samples in each annealing temperature group are plotted in separate two graphs

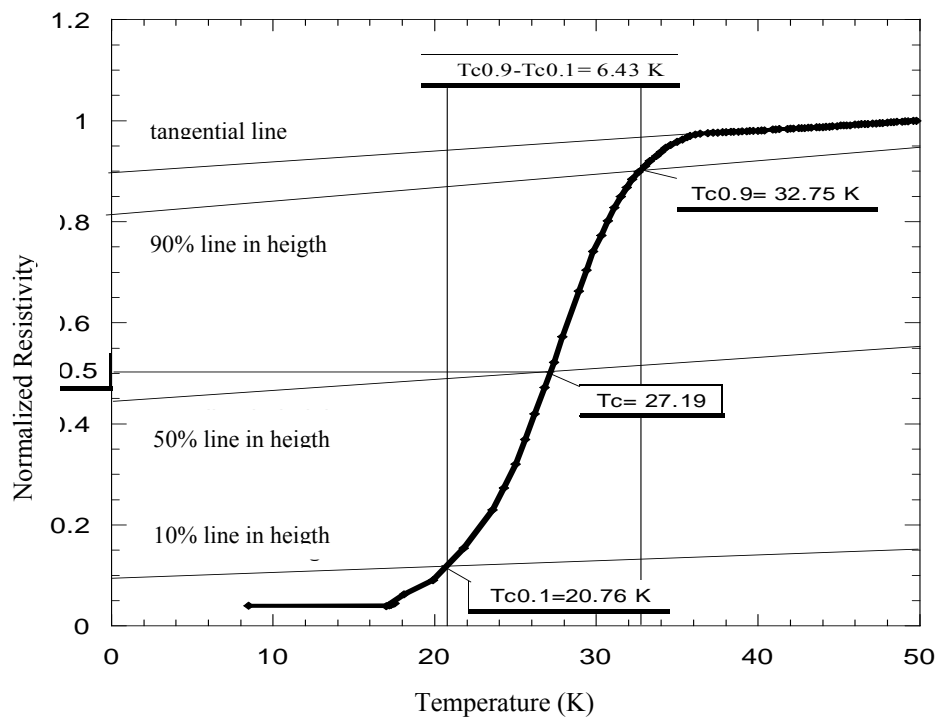
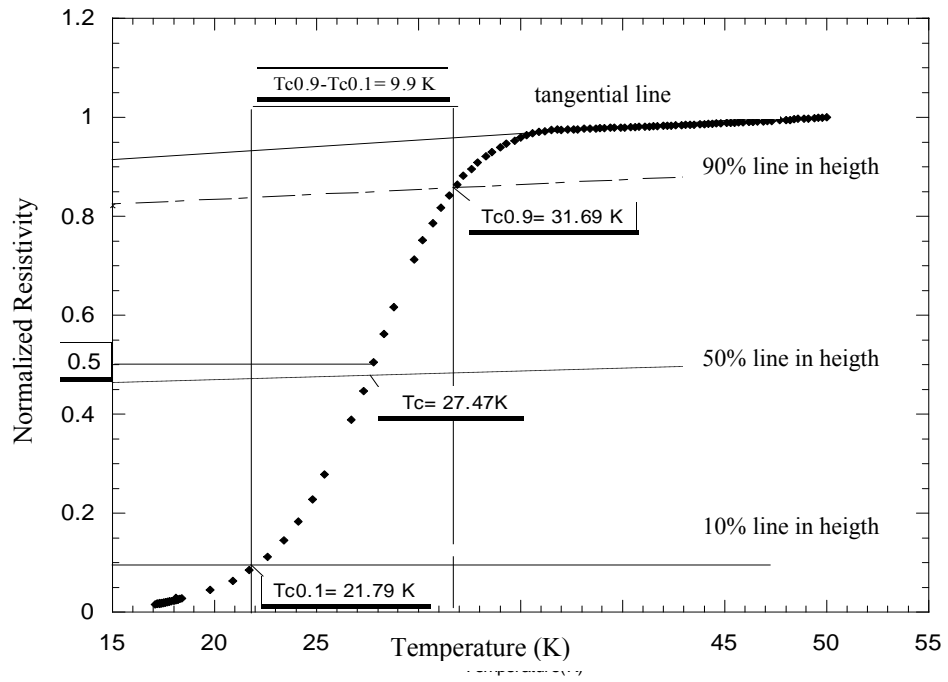


Figure 4.6 Method of  $T_c$ ,  $\Delta T_c$  Determination

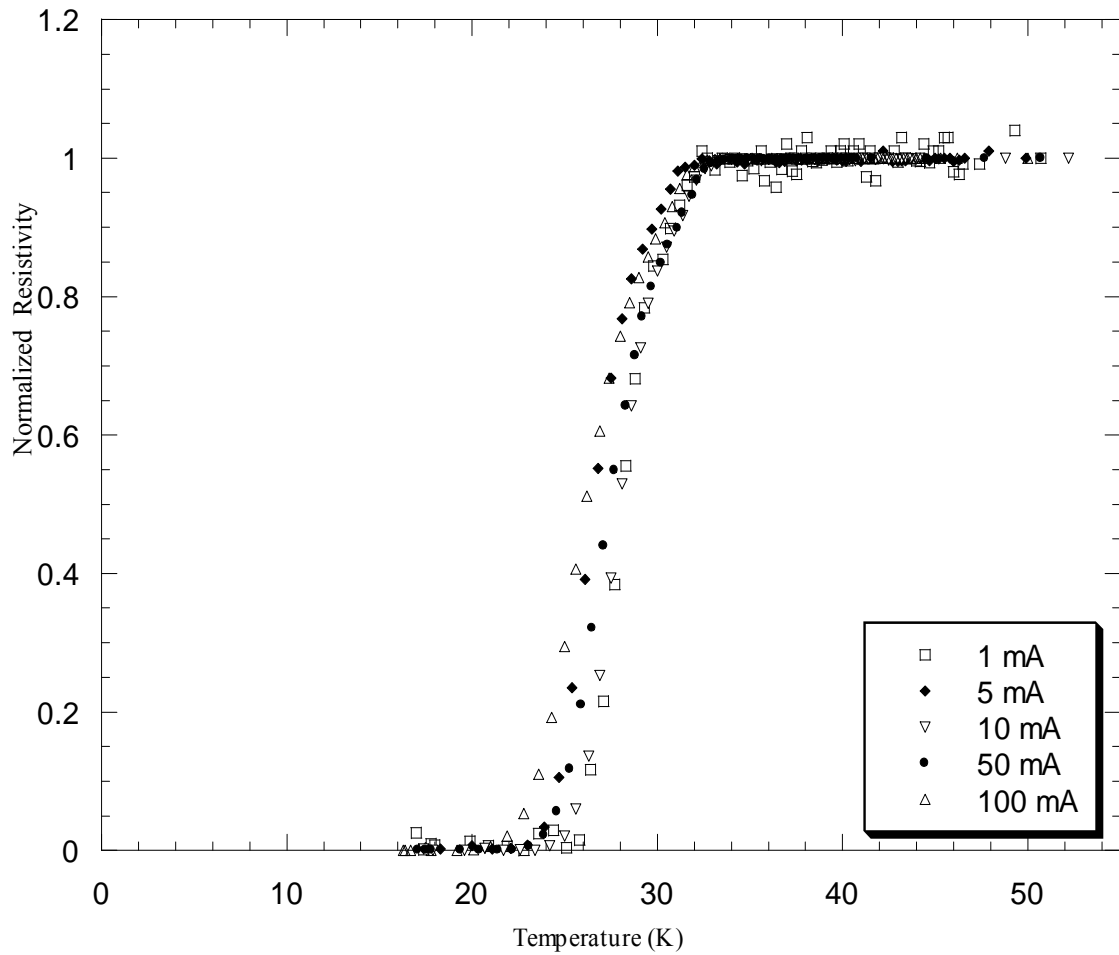


Figure 4.7 Resistivity-Temperature Results of Sample 400

Applied Current	$T_c$ (K)	$T_{c\text{ onset}}$ (K)	$\Delta T_c$ (K)	$T_{c0.1}$ (K)	$T_{c0.9}$ (K)
1 mA	28.1	32.42	4.75	26.26	31.01
5 mA	26.46	32.19	1.96	24.27	26.66
10 mA	27.82	33.13	5.5	25.87	30.92
50 mA	27.43	33	5.92	25	30.92
100 mA	25.97	32.42	6.7	23.54	30.24

Table 4.2 The  $T_c$  values of sample 400

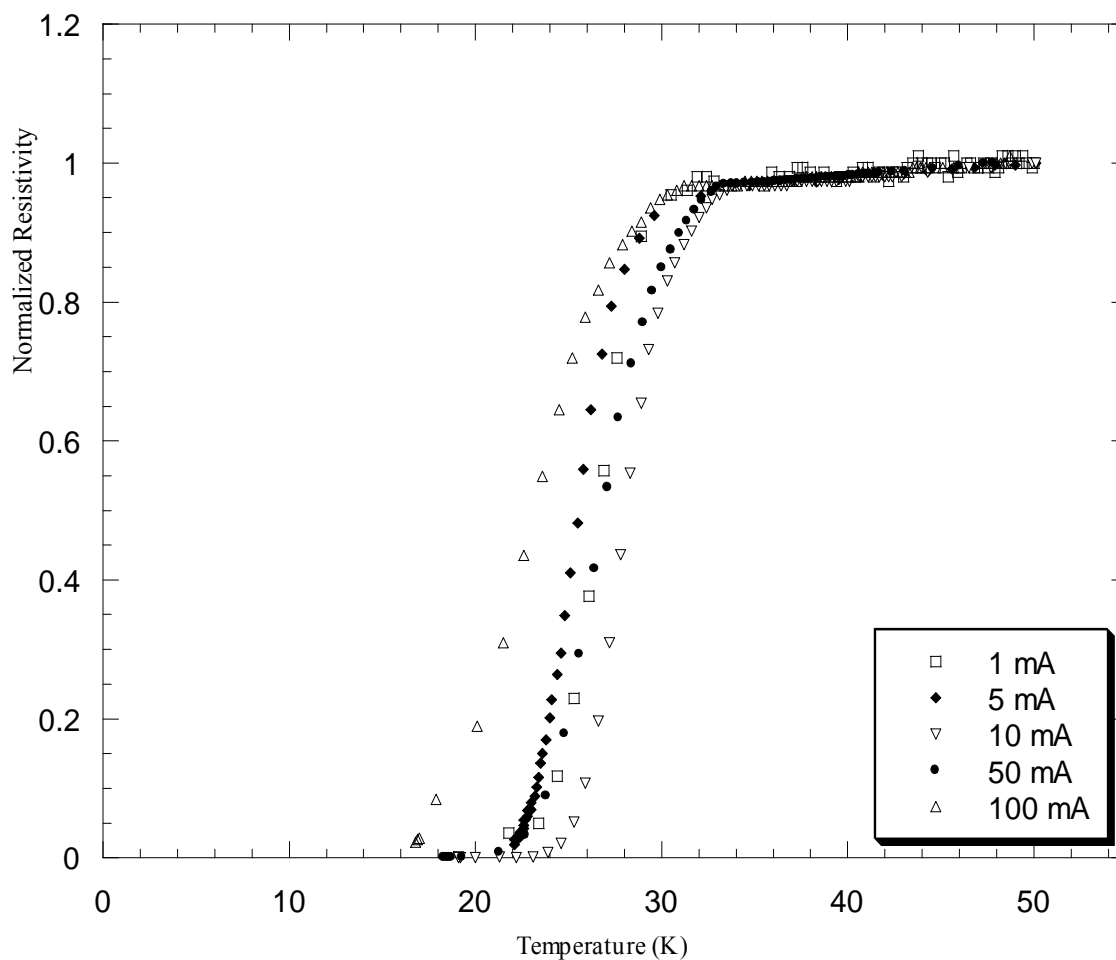


Figure 4.8 Resistivity-Temperature Results of Sample 405

Applied Current	$T_c$ (K)	$T_{c \text{ onset}}$ (K)	$\Delta T_c$ (K)	$T_{c0.1}$ (K)	$T_{c0.9}$ (K)
1 mA	26.55	31.97	4.68	24.03	28.98
5 mA	25.49	34.63	5.15	23.25	28.4
10 mA	28	33.34	5.24	25.68	30.92
50 mA	26.54	33.10	6.6	23.93	30.53
100 mA	23.06	31.17	9.32	18.1	27.42

Table 4.3 The  $T_c$  values of sample 405

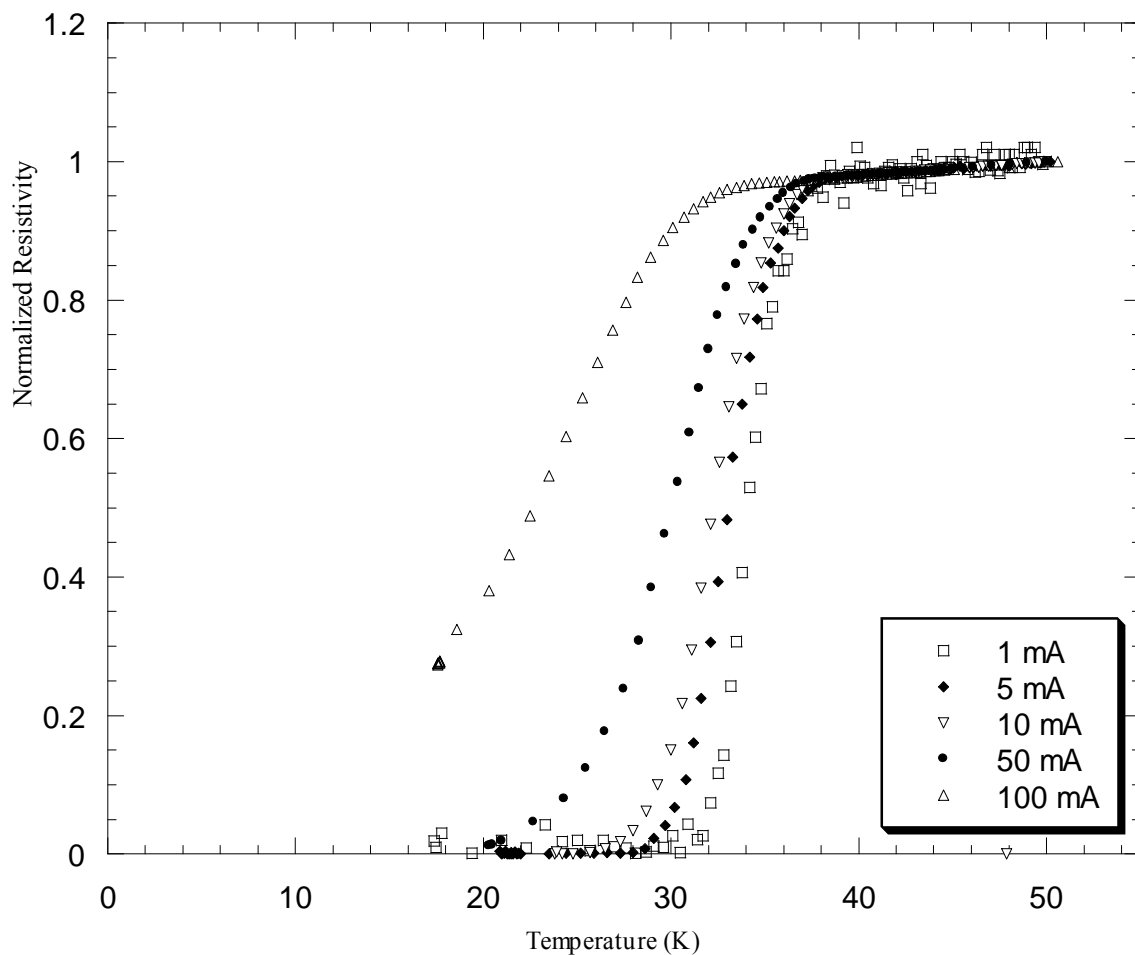


Figure 4.9 Resistivity-Temperature Results of Sample 410

Applied Current	$T_c$ (K)	$T_{c\ onset}$ (K)	$\Delta T_c$ (K)	$T_{c0.1}$ (K)	$T_{c0.9}$ (K)
1 mA	33.98	37.62	4.25	32.76	37.01
5 mA	33	38.21	5.01	30.64	35.65
10 mA	32.19	38.33	6.18	29.30	35.18
50 mA	29.93	36.89	9.11	24.6	33.71
100 mA	22.37	34.3	Not applicable	Not applicable	29.4

Table 4.4 The  $T_c$  values of sample 410

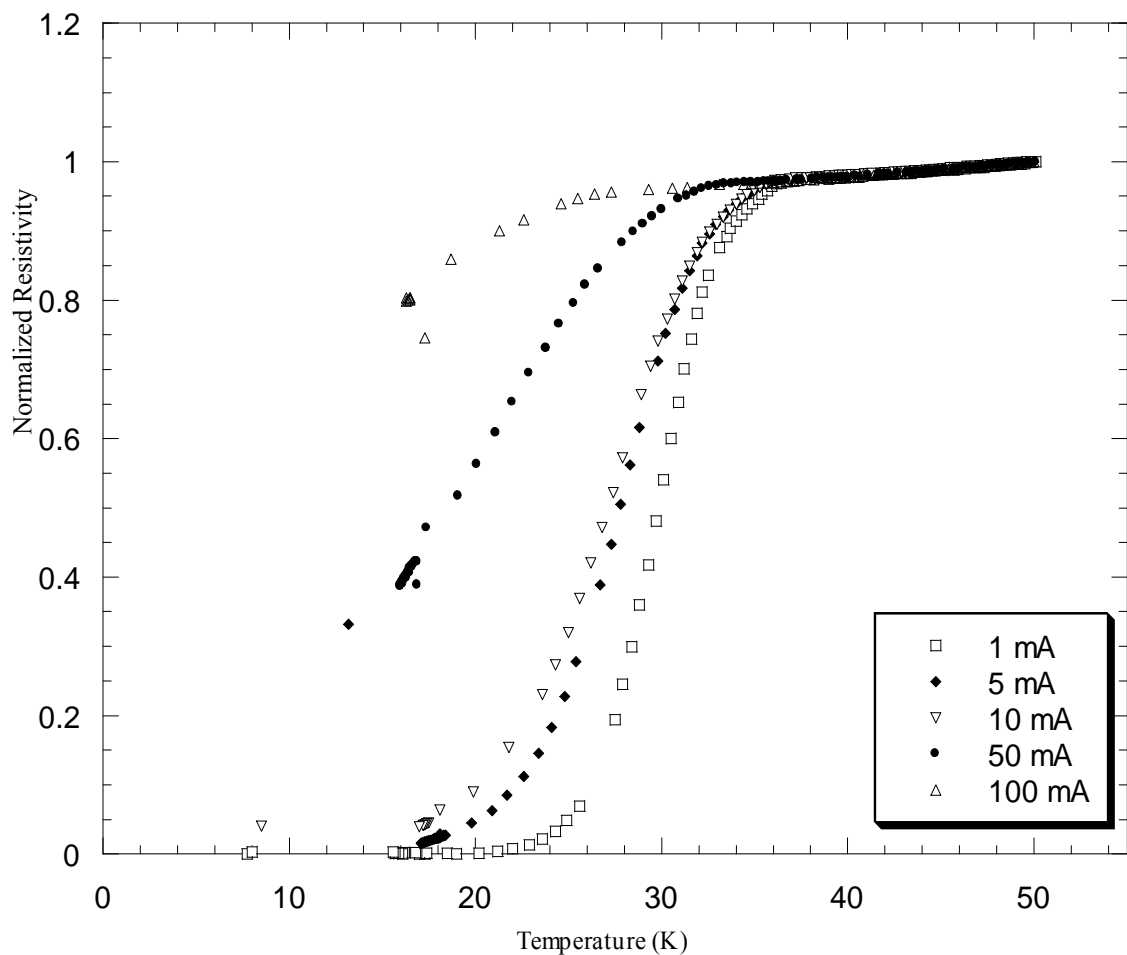


Figure 4.10 Resistivity-Temperature Results of Sample 415

Applied Current	$T_c$ (K)	$T_{c\ onset}$ (K)	$\Delta T_c$ (K)	$T_{c0.1}$ (K)	$T_{c0.9}$ (K)
1 mA	29.71	36.69	6.42	26.35	32.77
5 mA	27.47	35.78	9.9	21.79	31.69
10 mA	27.19	36.4	6.43	20.76	32.75
50 mA	17.34	33	Not applicable	Not applicable	Not applicable
100 mA	Not applicable	26.22	Not applicable	Not applicable	Not applicable

Table 4.5 The  $T_c$  values of sample 415

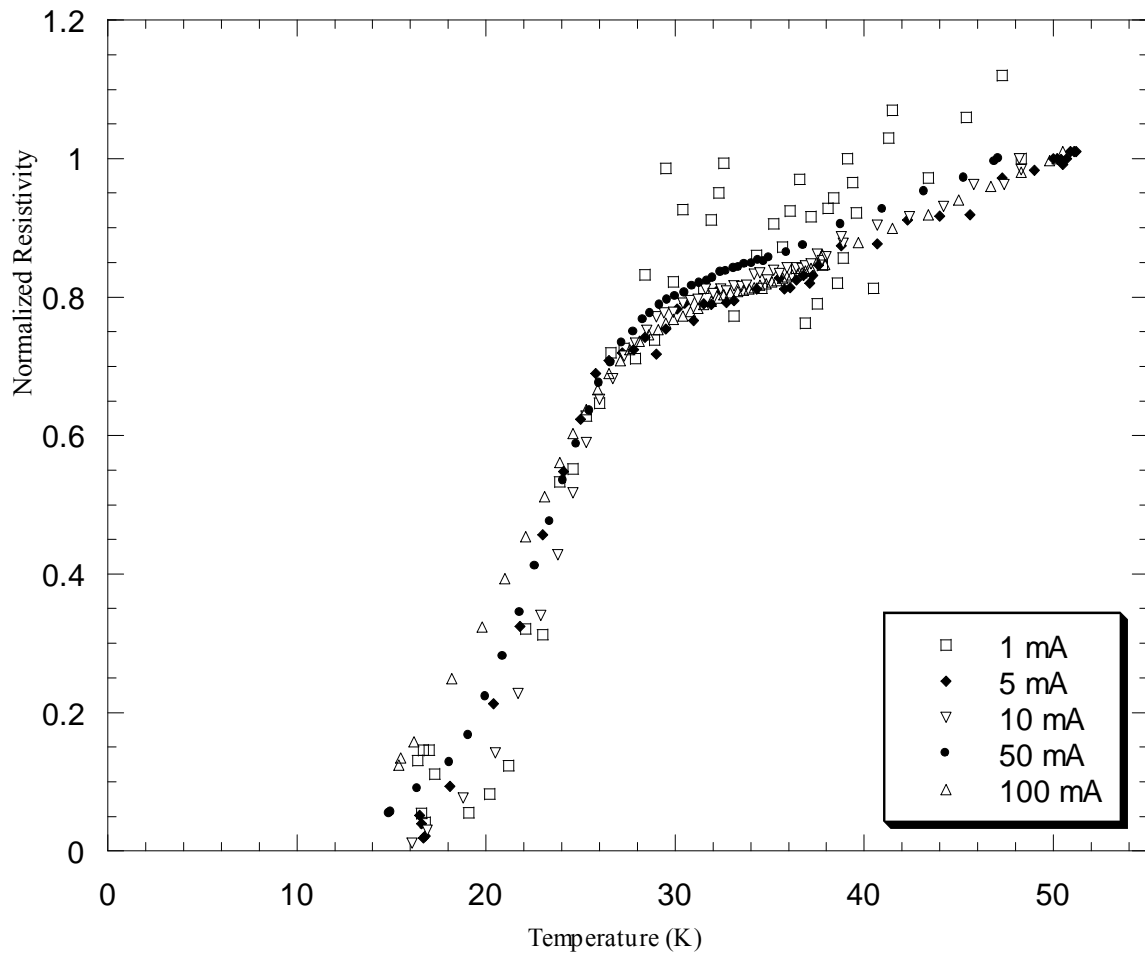


Figure 4.11 Resistivity-Temperature Results of Sample 420

Applied Current	$T_c$ (K)	$T_{c \text{ onset}}$ (K)	$\Delta T_c$ (K)	$T_{c0.1}$ (K)	$T_{c0.9}$ (K)
1 mA	22.67	27.99	6.14	19.09	25.23
5 mA	21.79	26.55	8.24	16.46	24.7
10 mA	22.67	28.50	7.78	17.86	25.64
50 mA	21.81	29.41	10.06	15.4	26.02
100 mA	19.46	28.69	Not applicabl	Not applicable	25.1

Table 4.6 The  $T_c$  values of sample 420

In type II superconductors vortex states formation below  $T_{c \text{ onset}}$  occur not only in the case of applied external magnetic field but also by the magnetic fields of electrical currents pass through it. The magnetic field in the vortices acts on the current with a Lorentz force. The current acts in opposite direction with the same force that consecutively leads dissipative losses and voltage drop in the superconductor. The main dissipation mechanism is the scattering of the normal-phase electrons by the thermal lattice vibrations. This results with Joule losses. Another mechanism is the thermal mechanism of dissipation in which the vortex motion is accompanied by energy absorption in a region of the forward boundary of the vortex. Such a thermal gradients and heat flow cause energy dissipation (Kresin and Wolf, 1990).

As a result of these energy dissipation mechanisms increasing current in the resistivity measurement broadens the resistivity versus temperature curves and beyond some critical current zero resistance cannot be attained. This broadening is also observed in our measurement depicted through Fig. 4.7 to 4.11. The deviations from this tendency in figure 4.7 for 10 mA, in Fig. 4.8 for 1 mA and in Fig. 4.11 for 5, 10 and 50 mA are possible due to the thermal contact problems between the cold head and sample. In the figure 4.9 superconducting transition for 100 mA and in figure 4.10 that for 50 and 100 mA is incomplete.

The normalized resistivity-temperature curves given in the previous pages illustrate a general tendency of decrease in the critical current with increasing Mg concentration. High porosity of the samples prepared at 400 °C seems to prevent the passage of currents even around 50 mA and 100 mA for 10% and larger values of Mg addition. In the case of lower values of Mg concentration current can percolate through small linked cross sections. Presence of large cluster of Mg seams to be one factor reducing the net cross section to the percolation paths of supercurrents.

Other characteristic depicted by the curves is that with increasing Mg concentration, Mg dominates the resistivity behavior in the normal state and broadens the resistivity curve. Latter one will be more closely examined at the last parts of the chapter.

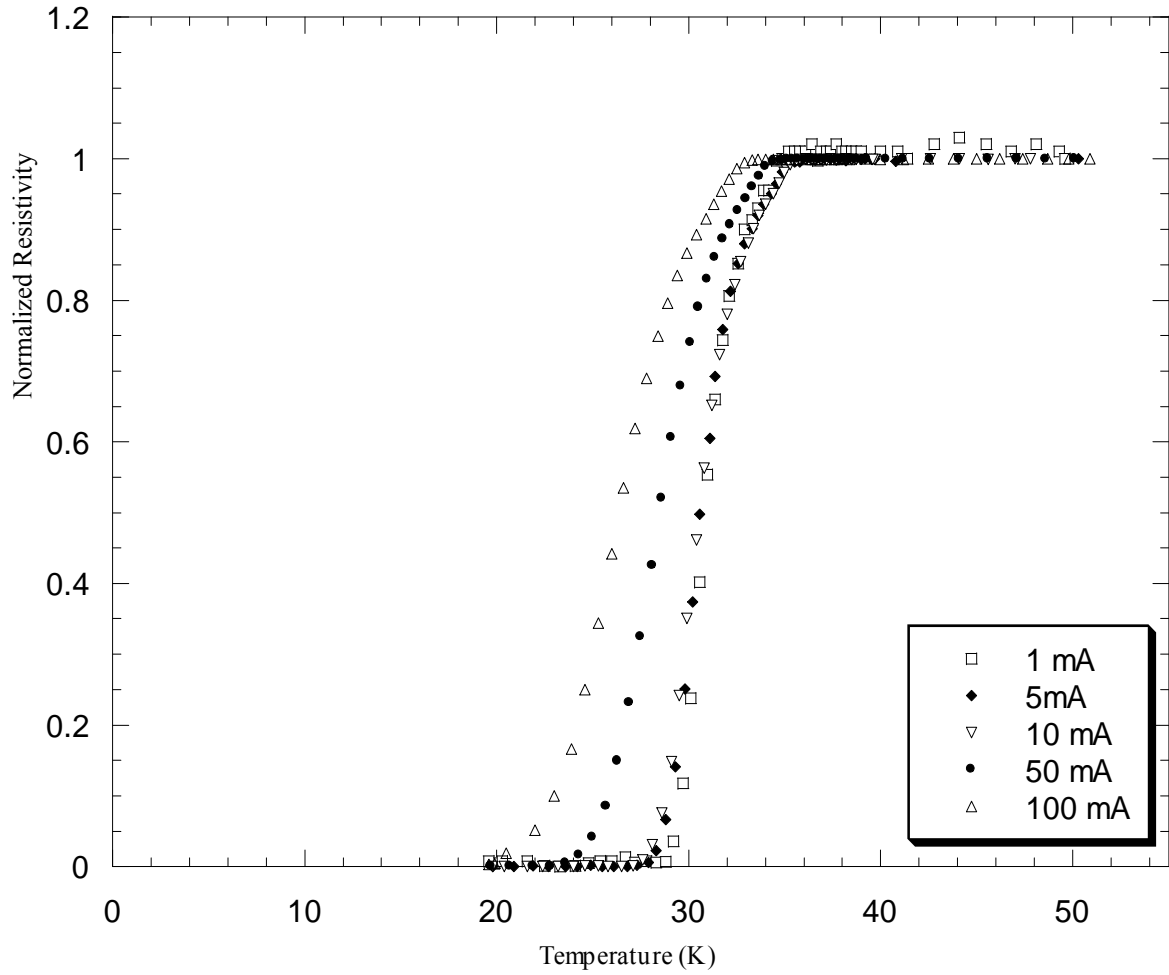


Figure 4.12 Resistivity-Temperature Results of Sample 500

Applied Current	$T_c$ (K)	$T_{c\ onset}$ (K)	$\Delta T_c$ (K)	$T_{c0.1}$ (K)	$T_{c0.9}$ (K)
1 mA	30.82	35.20	3.59	29.27	32.86
5 mA	30.63	35.23	4.56	28.59	33.15
10 mA	30.43	35.57	4.95	28.30	33.25
50 mA	28.39	34.41	6.98	25.1	32.08
100 mA	26.26	32.57	8.93	21.6	30.53

Table 4.7 The  $T_c$  values of sample 500

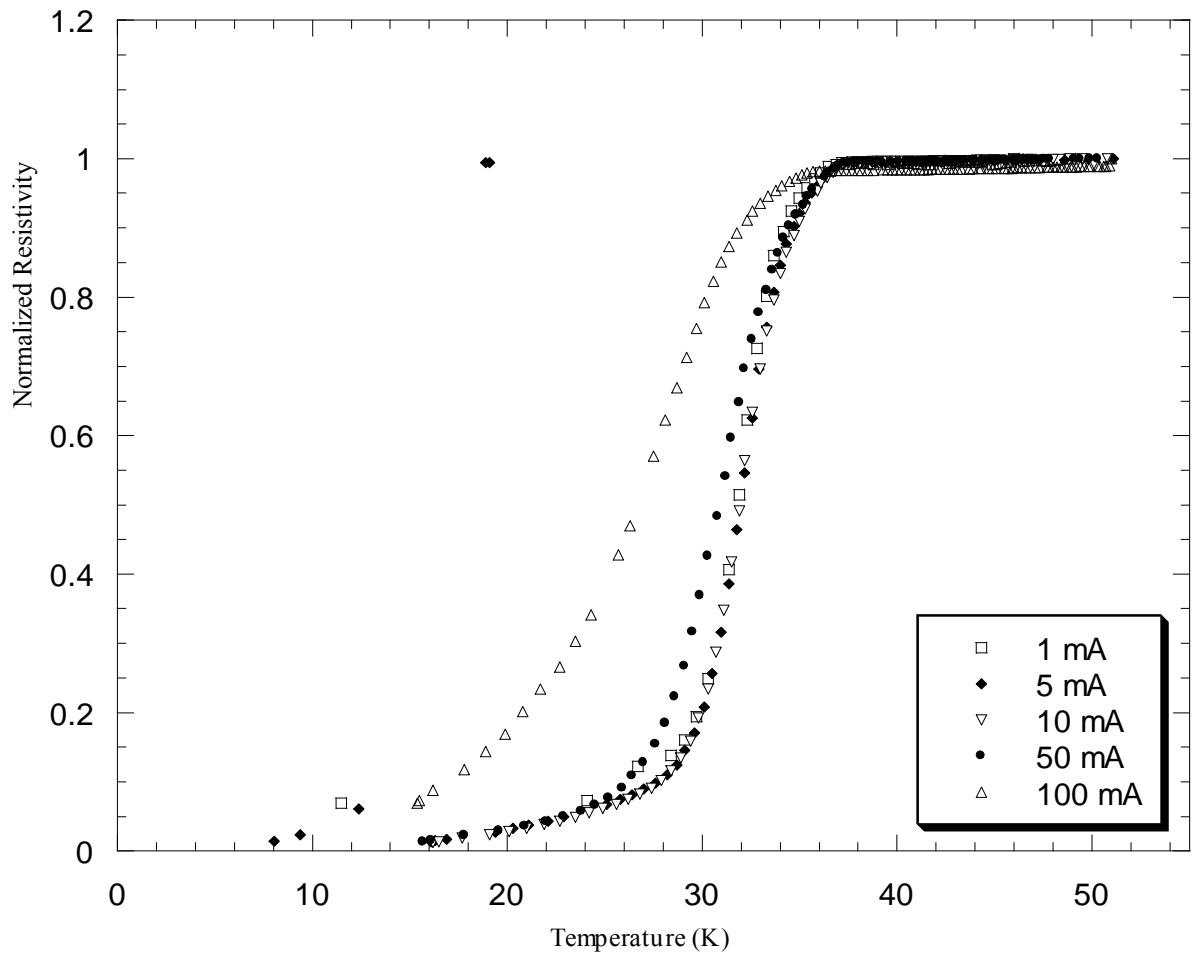


Figure 4.13 Resistivity-Temperature Results of Sample 505

Applied Current	$T_c$ (K)	$T_{c\ onset}$ (K)	$\Delta T_c$ (K)	$T_{c0.1}$ (K)	$T_{c0.9}$ (K)
1 mA	31.89	37.13	6.17	27.9	34.07
5 mA	31.89	37.54	6.26	28.1	34.36
10 mA	31.89	37.33	6.4	27.96	34.36
50 mA	30.87	37.22	8.15	26.21	34.36
100 mA	26.80	35.70	15.72	16.89	32.60

Table 4.8 The  $T_c$  values of sample 505

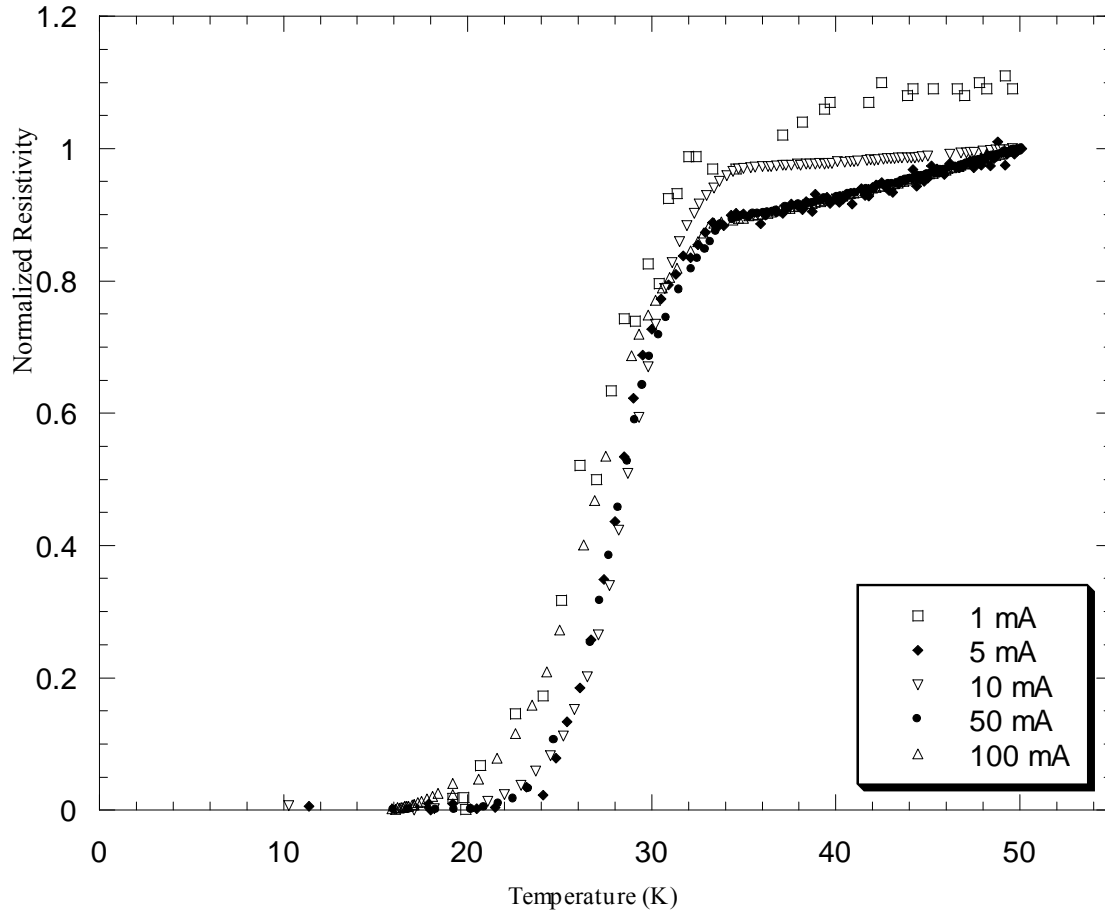


Figure 4.14 Resistivity-Temperature Results of Sample 510

Applied Current	$T_c$ (K)	$T_{conset}$ (K)	$\Delta T_c$ (K)	$T_{c0.1}$ (K)	$T_{c0.9}$ (K)
1 mA	25.65	37.13	7.77	21.40	29.17
5 mA	27.84	37.36	5.35	24.92	30.27
10 mA	28.32	37.22	5.87	25.53	31.24
50 mA	27.84	34.06	7.04	24.32	31.36
100 mA	26.50	33.21	8.62	21.65	30.27

Table 4.9 The  $T_c$  values of sample 510

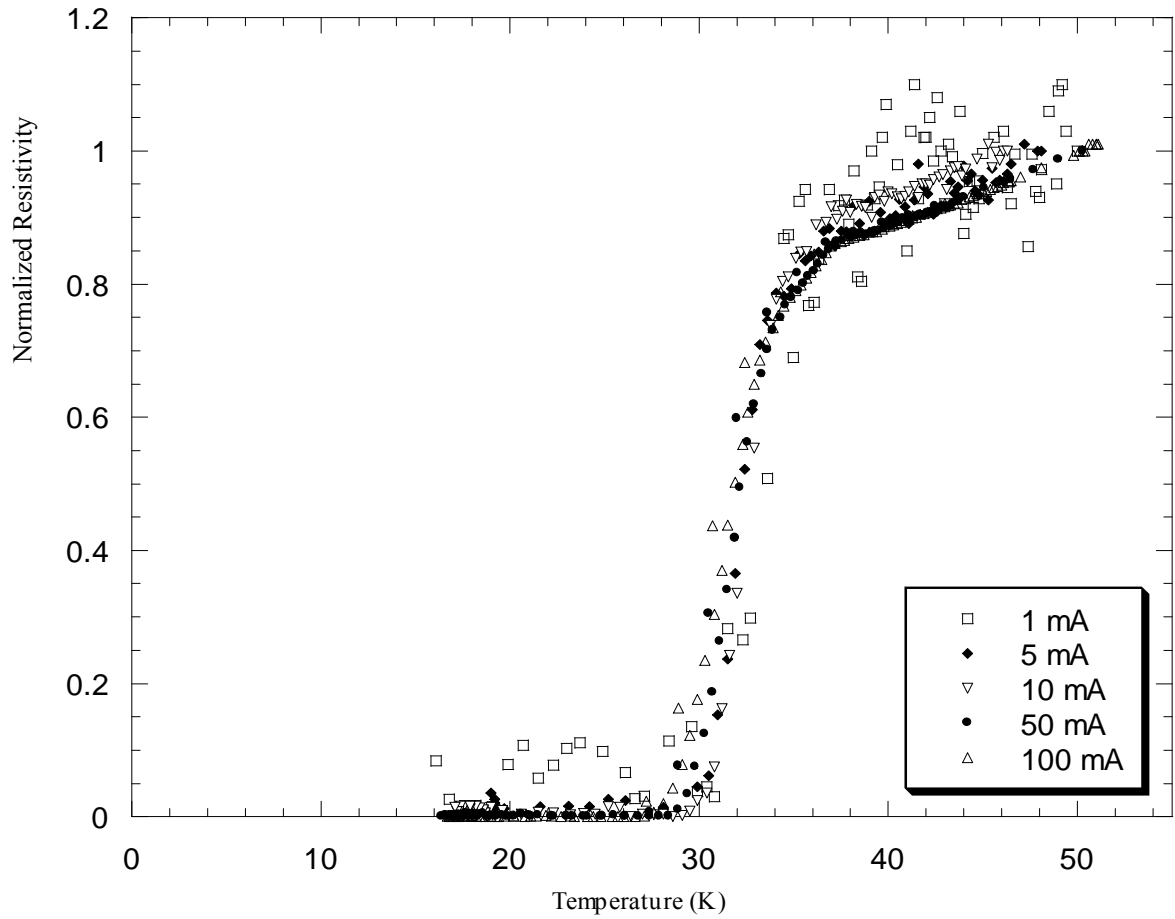


Figure 4.15 Resistivity-Temperature Results of Sample 515

Applied Current	$T_c$ (K)	$T_{c\ onset}$ (K)	$\Delta T_c$ (K)	$T_{c0.1}$ (K)	$T_{c0.9}$ (K)
1 mA	32.96	36.26	7.29	28	35.29
5 mA	32.90	36.28	2.97	31.47	34.44
10 mA	32.50	36.15	3.31	30.80	34.11
50 mA	31.79	36.55	3.98	29.85	33.83
100 mA	31.14	36.75	5.02	29.04	34.06

Table 4.10 The  $T_c$  values of sample 515

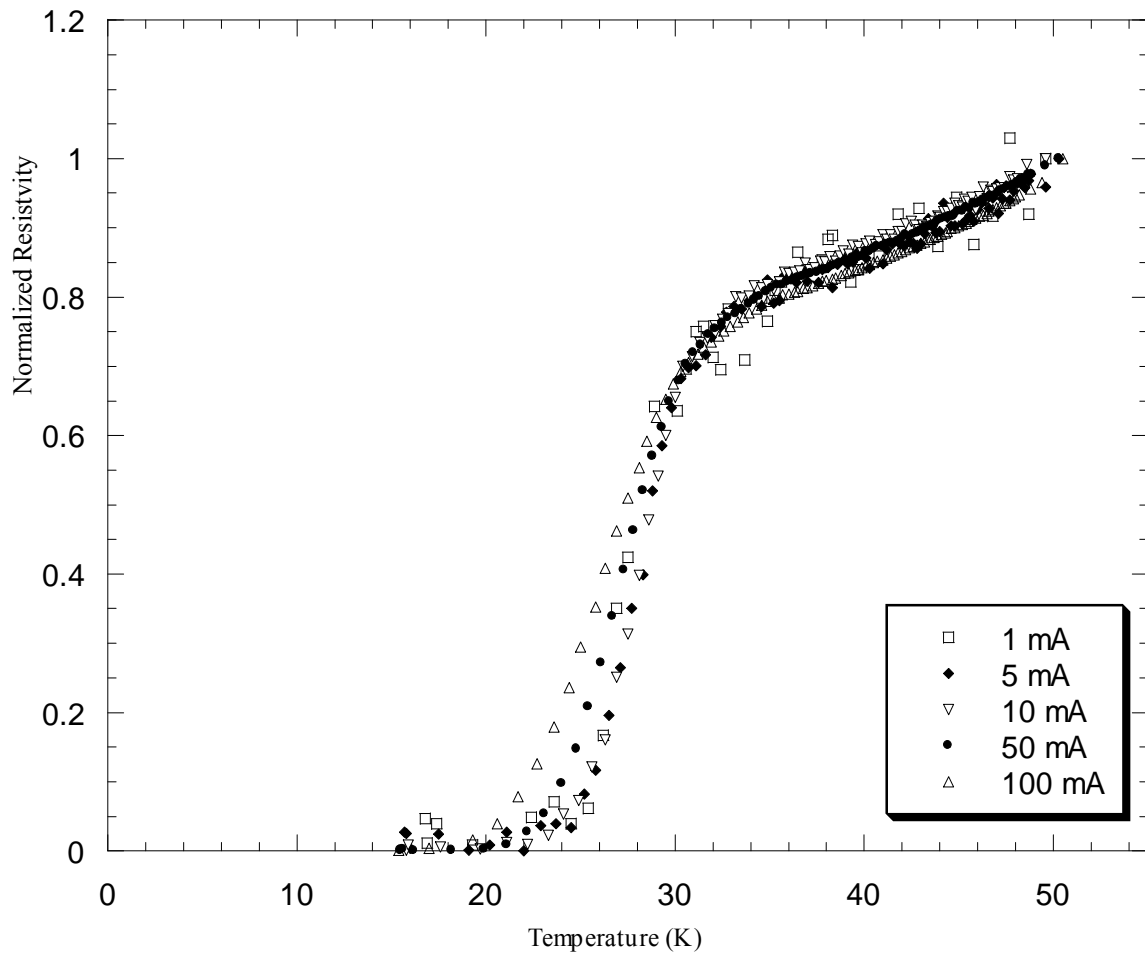


Figure 4.16 Resistivity-Temperature Results of Samples 520

Applied Current	$T_c$ (K)	$T_{c\ onset}$ (K)	$\Delta T_c$ (K)	$T_{c0.1}$ (K)	$T_{c0.9}$ (K)
1 mA	26.87	31.06	5.15	24.12	29.27
5 mA	27.62	32.77	5.92	23.83	29.75
10 mA	27.81	33.15	5.43	24.90	30.33
50 mA	25.87	32.47	7.28	22.86	30.14
100 mA	24.51	33.54	9.03	20.33	29.56

Table 4.11 The  $T_c$  values of sample 520

The interruptions of superconducting transition in the resistivity-temperature measurements given in Fig. 4.9 and 4.10 for 50 and 100 mA were not observed in the samples prepared by a 500 °C heat treatment. These two figures indicate that a 100 °C increase in heat treatment leads to an improvement in critical current of the samples. That increase may be caused by an increase in the MgO concentration that acts as pinning center, grain refinement and better grain linkages.

The presence of MgO with small grain sizes has been suggested as a possible pinning center (Zhao et al., 2002) Pinning centers prevent the motion of vortex states and so the energy dissipation to some extent.

Table 3.1 and the SEM images indicate a consolidation and better grain linkage with increasing heat treatment. Such an increase in the grain linkage has been reported in many studies as previously mentioned in this text. It decreases weak link problems.

Although usually grain refinements in MgB<sub>2</sub> occur by drawing and rolling processes, the results obtained from examination of SEM image suggest presence of such a refinement in the 500 °C. Grain refinement increases grain boundary pinning which in turn increases pinning enhancement (Zhoa et al, 2002).

The resistivity-temperature results given through Fig. 4.12 to 4.16 illustrate the effect of increasing Mg concentration on transition. The increases in the slope of the curves in normal state arise from relatively lower resistance of Mg with respect to MgB<sub>2</sub>. In addition Table 4.7, 4.8 and 4.10 point out a tendency of improvement in critical temperature. While aberration from this tendency in the resistivity-temperature results of the sample including 10 wt% excess Mg probably a result of thermal contact problem in the measurements, that for the sample with 20 wt% excess Mg most likely due to the weak link problems aroused by large clusters of Mg. The latter case will further examined after Fig. 4.17 and 4.18 that illustrates the effect of Mg concentration on resistive transition behavior.

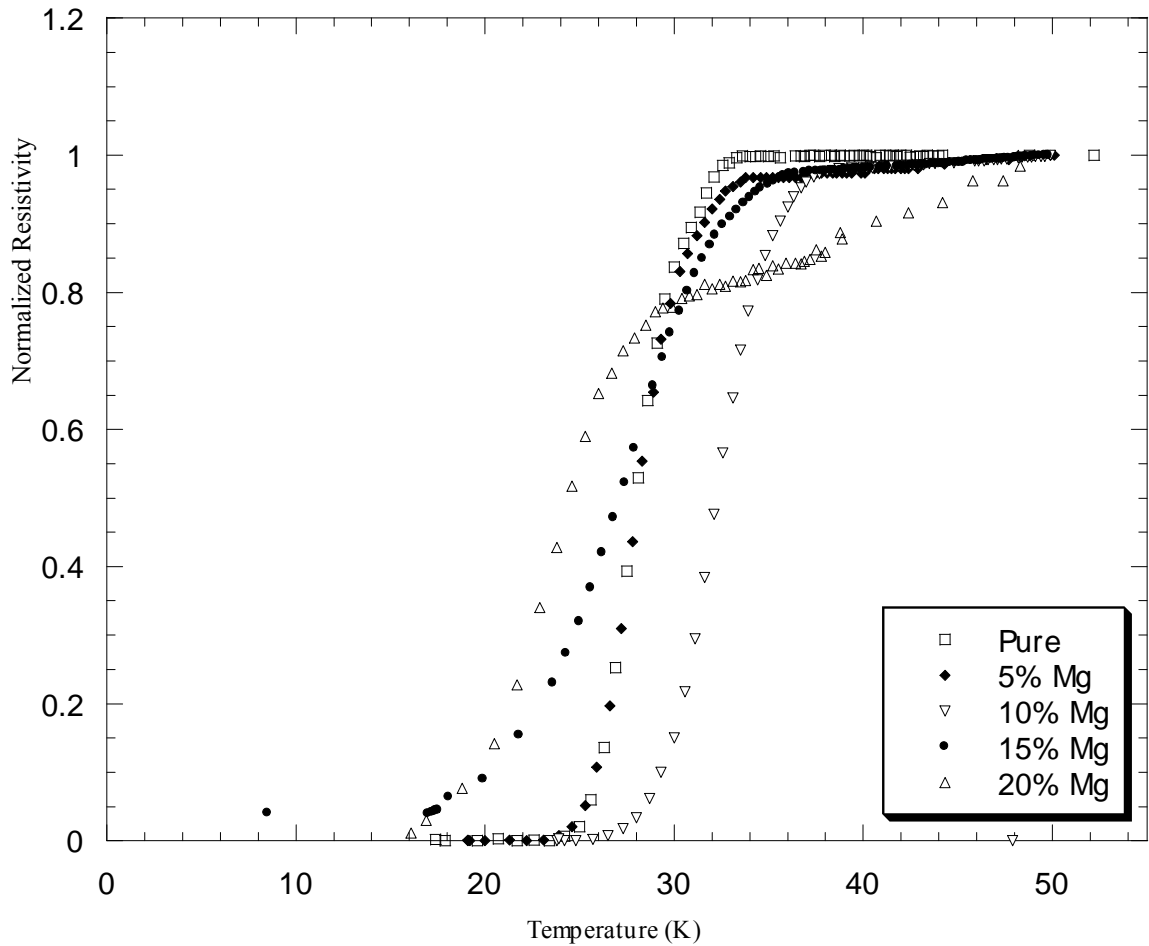


Figure 4.17 10 mA Resistivity-Temperature results of 400 °C heat-treated pellets.

Applied Current	$T_c$ (K)	$T_{c\text{ onset}}$ (K)	$\Delta T_c$ (K)	$T_{c0.1}$ (K)	$T_{c0.9}$ (K)
Pure	27.82	33.13	5.5	25.87	30.92
+5% Mg	28	33.34	5.24	25.68-	30.92
+10% Mg	32.19	38.33	6.18	29.30	35.18
+15% Mg	27.19	36.4	6.43	20.76	32.75
+20% Mg	22.67	28.50	7.78	17.86	25.64

Table 4.12 The  $T_c$  values of the samples

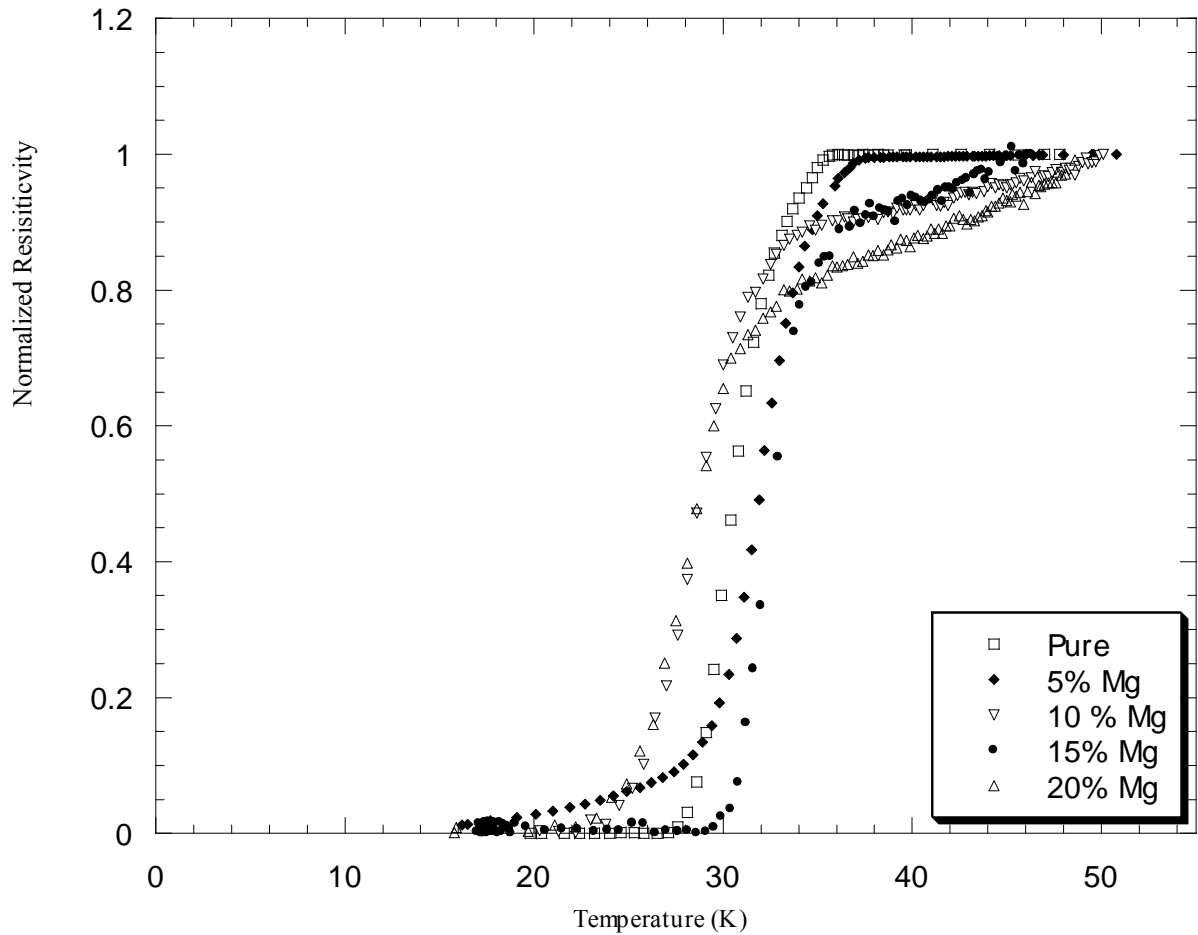


Figure 4.18 10 mA resistivity-temperature results of 500 °C heat-treated pellets.

Applied Current	$T_c$ (K)	$T_{c\ onset}$ (K)	$\Delta T_c$ (K)	$T_{c0.1}$ (K)	$T_{c0.9}$ (K)
Pure	30.43	35.57	4.95	28.30 K	33.25 K
+5% Mg	31.89	37.33	6.4	27.96 K	34.36 K
+10% Mg	28.32	37.22	5.87	25.53 K	31.24 K
+15% Mg	32.50	36.15	3.31	30.80 K	34.11 K
+20% Mg	27.81	33.15	5.43	24.90 K	30.33 K

Table 4.13 The  $T_c$  values of the samples

Most evident effect of increasing Mg constituents in the Fig. 4.17 and 4.18 is an increase in slope of the resistivity curve above the transition temperature. In normal state the resistivity-temperatures graphs of samples including excess Mg has a slope strongly depends on the Mg concentration and when the superconducting transition begin this slope suddenly increases. The change in the slope above the  $T_{c \text{ onset}}$  results from temperature dependence of Mg resistance. Mg has relatively lower resistance compared to  $\text{MgB}_2$  and with increasing concentration of Mg the resistivity of the curve above  $T_{c \text{ onset}}$  suppressed. Under the  $T_{c \text{ onset}}$  current percolate through superconducting  $\text{MgB}_2$  phases and slope in this part mainly determined by superconducting  $\text{MgB}_2$  phases and consequently by their grain connectivity, grain size, porosity and purity. The broadening is an undesired effect especially when the  $T_{c \text{ zero}}$  decreases considerably.

As revealed from graphics a 100 °C increase in heat treatment in this temperature range leads an improvement in  $T_c$  and  $T_{c \text{ onset}}$  values and a 0.55 K decreases  $\Delta T_c$  for pure samples. This is probably a result of increases in grain connectivity and better fuse of Mg in empty spaces by decreasing porosity of the sample. For 400 °C heat-treated samples this increase in  $T_c$  continues up to 10% Mg addition. The value of the improvement is around 4.37 K. On the other hand  $T_{c \text{ onset}}$  gets higher values up to 15% Mg addition and maximum value is reached for the sample with 10% excess Mg. The amount of increase in  $T_{c \text{ onset}}$  for sample 410 relative to that of pure sample is 5.2K. Similar case is also valid for samples prepared by 500 °C heat-treatment with some exceptions. For these samples  $T_c$  continue to increase up to 15% Mg addition. The maximum magnitude of the increase in the  $T_c$  is obtained for sample 515 and that in the  $T_{c \text{ onset}}$  is reached for sample 505. The magnitudes of increases are about 2.07 K and 1.76 K, respectively. Although  $T_{c \text{ onset}}$  value is better for 500 °C heat-treated one among the pure samples, in the case of Mg substitution a best value is obtained for the sample 410. While  $\Delta T_c$  increases with increasing concentration of Mg for the 400 °C heat-treated sample, fluctuate with increasing Mg concentration for the 500 °C heat-treated samples. The reason of these fluctuations is probably a thermal contact problem with the sample and cold heat.

In spite of the slight increase of  $T_c$  in sample 410 relative to sample 400, vice versa is valid for  $T_{c \text{ zero}}$  for these samples. The reason of this relative reduction in  $T_{c \text{ zero}}$  might be inhomogeneous grain distribution with different  $T_c$  values. Different grains can have different  $T_c$  values due to the dimensions of  $\text{MgB}_2$  and the thickness of Mg layers around them. In the case of direct junction between a superconductor and a normal

metal, the overlap of the wave functions causes the density  $n_s$  of electron pairs to differ in the neighborhood of the surface from its value in the bulk. The presence of such an interface causes leakage of some quasi particles into superconductor and leakage of some cooper pairs to the normal metal. This effect is called as proximity effect. The proximity effect generally results with the suppression of the superconducting properties like  $T_c$ . (in some rare cases enhancement is possible and these are called as inverse proximity effect) After some characteristic thickness of normal layer no further reduction in  $T_c$  of superconductor is occur and if the thickness of the superconductor larger than the coherence length, irrespective of the normal layer thickness  $T_c$  does not show considerable change. In our samples Mg is not distributed homogenously in the sample, as a result of this we have many parts in the sample with a variety of  $T_c$  values. Hence all of these grains become superconductor at different temperature and a broadening result. According to this the broadening observed in transition of our samples can be caused by proximity effect. Even with resistivity measurements it is not possible to examine the transition behavior of the whole substance, still the broadening can attributed to the proximity effect and disorder. The hypothesis seems to be supported by the explanation of relative superconducting transition broadening in magnetization measurements of the  $MgB_2/Al$  and  $MgB_2/Mg$  composite pellets with the proximity effect and disorder (Sharoni et al., 2001, Dunand, 2001). Compared to composite forms all the part of the pure substance past to superconducting state almost at the same temperature. This is the reason of the sharp transition and higher  $T_{c\ onset}$ . in the sample 400. The higher value of  $T_c$  and  $T_{c\ onset}$  in the samples containing excess Mg might be due to the formation of percolation paths by presence of thin layer of Mg between superconducting  $MgB_2$  grains. This layer can show superconducting properties as a result of proximity effect. Existence of such paths can increase  $T_c$  and  $T_{c\ onset}$ , which is lower in pure sample 400 because of large distances between grains and the interruption of supercurrent through such a kind of large distances.

20% Mg addition suppresses both the  $T_c$  and  $T_{c\ onset}$  values of samples for both 400 °C and 500 °C heat treatment with respect to pure samples subjected to similar heat treatments. In addition a broadening in  $\Delta T_c$  is observed for these samples. While the magnitude of this broadening is 2.28 K for 400 °C, that for 500 °C is 0.48 K.

## CHAPTER 5

### CONCLUSIONS

It is difficult to use  $\text{MgB}_2$  in bulk applications due to its brittleness. Fortunately, it is possible to improve the mechanical properties either by cladding of  $\text{MgB}_2$  cores with a ductile metallic sheaths or by the fabrication of a metal matrix composites. In this study, we have used the latter approach. By doing so, we hope the benefit from the heat and electrical conductivity of the metal in the case of localized break down in the superconductivity of the  $\text{MgB}_2$  phase and improve the crack arrest and toughness of the bulk material.

The XRD and SEM studies indicate the possible presence of small quantities of second phases like  $\text{MgO}$ ,  $\text{MgB}_4$ ,  $\text{MgB}_6$ . While presence of  $\text{MgB}_4$  and  $\text{MgB}_6$  may cause weak link problems, the data point to the source of these phases as commercial powders and so they are not main source of the broadening in the superconducting transition of our samples. Existing  $\text{MgO}$  can act as a pinning center and concurrently can enhance the superconducting critical current. Increasing concentration of  $\text{MgO}$  with increasing  $\text{Mg}$  concentration and heat might be one of the factors enhancing the supercurrent in the 500 °C heat-treated samples relative to that of 400 °C. The resistivity curves for various currents imply a general tendency of decrease in the critical current with increasing  $\text{Mg}$  concentration. High porosity of the samples prepared at 400 °C seem to prevent the passage of currents even around 50 mA and 100 mA for 10% and larger values of  $\text{Mg}$  addition. On the other hand lower currents can be superconducted through small linked cross sections. Presence of large cluster of  $\text{Mg}$  seams to be one factor interrupting the net cross section of the percolation paths of supercurrents.

Although the  $\text{Mg}$  did not diffuse deep in to whole the grain boundaries homogenously, the presence of it up to some extent increases the  $T_c$  of the samples due to the formation of percolation paths as a result of proximity effect.

A 100 °C increases in heat treatment in the temperature range leads an improvement in  $T_c$  and  $T_{c \text{ onset}}$  values and a decrease in  $\Delta T_c$  for pure samples for 10 mA resistivity measurements. This is probably a result of increases in grain connectivity and better fuse of  $\text{Mg}$  in empty spaces by decreasing the porosity of the samples. In our temperature range increasing heat treatment enhanced the grain linkage and concomitantly decreases the weak link problems resulting from poor grain connectivity and highly porous structure of the pellets. Furthermore the SEM images and the ratio of

empirical density to theoretical density denote a decrease in porosity with increasing Mg concentration and temperature. While an increase in  $T_c$  continues up to 10% Mg addition for the lower heat treatment, it continues up to 15% Mg addition for the higher heat treatment and the best value is attained by 500 °C heat treated one. In addition while  $\Delta T_c$  increases with increasing concentration of Mg for the 400 °C heat-treated sample, fluctuate with increasing Mg concentration for the 500 °C heat treated samples. The reason of these fluctuations is probably a thermal contact problem with the sample and cold heat. One of the feasible sources for the broadening of superconducting transition in the resistivity-temperature measurements is the proximity effect. MgB<sub>2</sub> grains in contact with the Mg have different  $T_c$  according to their relative thickness to each other, coherence length and characteristic thickness of normal state. The presence of the grain with different  $T_c$  on the percolation paths results in a broadening of superconducting transition in the resistivity curves. The presence of large areas of Mg and disorder is the supporting factor in the broadening.

Compared to composite forms, all the part of the entire pure substance past to superconducting state almost at the same temperature. This is the reason of the sharp transition and higher  $T_{c \text{ onset}}$  in the pure samples. The higher value of  $T_c$  and  $T_{c \text{ onset}}$  in case of presence of extra Mg might be due to the formation of percolation paths by presence of thin layer of Mg between superconducting MgB<sub>2</sub> grains. This layer can show superconducting properties as a result of proximity effect and results in the formation of these paths.

Most evident effect of increasing Mg constituents in the samples is increasing slope of the resistivity curve at temperatures above the  $T_{c \text{ onset}}$ . This slope is directly correlated with the Mg concentration and temperature dependence of Mg resistance. Without Mg substitution resistivity curve follow a path with a zero slope and a very sharp superconducting transition occur. Under the  $T_{c \text{ onset}}$  current penetrate through superconducting MgB<sub>2</sub> phases and slope in this part mainly determined by superconducting MgB<sub>2</sub> phases and in turn with proximity effect, their grain connectivity, grain size, porosity, and distribution of impurities.

All the results indicates that beyond some Mg concentration further Mg addition suppresses both the  $T_c$  and  $T_{c \text{ onset}}$  values of samples for the both temperature like in the case of 20% Mg addition. In addition an extra broadening is observed for these samples. The broadening is an undesired effect especially when the  $T_{c \text{ offset}}$  decreases considerably.

Although the present data indicates an improvement in superconducting properties of the samples with increasing temperature in our range and Mg concentration to some extent, all these interpretations made by considering the existing resistivity curves do not lead a certain understanding of the superconducting transition mechanism and properties of the Mg/MgB<sub>2</sub> composite fabricated during this study. As pointed out before, resistivity curves may demonstrate the superconducting transition of only a small part of the whole sample. To obtain data corresponding to the superconducting transition of entire bulk, magnetization measurement should be carried out. The existing data only suggest a possible increase in  $T_c$  of sample annealed at a temperature around 500 °C with increasing Mg concentration up to some value between 15% and 20%, and an increase in critical current relative to samples annealed at 400 °C.

## APPENDIX

**Table A- 1 Characteristics of Mg**

Theoretical Density	1.738 gr/cm <sup>3</sup>
Atomic Weight	24.3050
Atomic Number	12
Molar Volume	14 cm <sup>3</sup>
Melting Point	650 °C
Boiling Point	1090 °C
Crystal Structure	Hexagonal Close-Packed
Hexagonal Lattice Parameters	a=320.94
	c=521.08
Superconduction Temperature	No data
Electrical Resistivity	440 μΩcm
Atomic Radius	Empirical radius 150 pm
	Calculated radius 145 pm
Young Modulus	45 GPa
Bulk Modulus	45 Gpa
Rigidity Modulus	17 GPa
Hardness	2.5

Data in the table obtained from web page

<http://www.webelements.com/webelements/elements/text/Mg>

**Table A-2 Characteristics of MgB<sub>2</sub>** (Buzea and Yamashita, 2001)

Parameter	Values
Formula Weight	45.93
Theoretical Density	$\rho = 2.625 \text{ g cm}^{-3}$
Melting Point	800 <sup>0</sup> C
Hexagonal Lattice Parameters	$a = 3.0855 \pm 0.0006 \text{ \AA}$
	$c = 3.522 \pm 0.002 \text{ \AA}$
Critical Temperature	$T_c = 39\text{--}40 \text{ K}$
Carrier Density	$n_s = 1.7\text{--}2.8 \times 10^{23} \text{ holes/cm}^3$
Penetration Depth	$\lambda(0) = 85\text{--}180 \text{ nm}$
Coherence Lengths	$\xi_{ab} = 3.7\text{--}12 \text{ nm}$
	$\xi_c = 1.6\text{--}3.6 \text{ nm}$
Pressure coefficient	$dT_c/dP = -11\text{--}2 \text{ K/GPa}$
Energy Gap	$\Delta(0) = 1.8\text{--}7.5 \text{ meV}$
Critical Current Densities	$J_c(4.2 \text{ K}, 0\text{T}) > 10^7 \text{ A/cm}^2$
	$J_c(4.2 \text{ K}, 4\text{T}) \sim 10^6 \text{ A/cm}^2$
	$J_c(4.2 \text{ K}, 10\text{T}) > 10^5 \text{ A/cm}^2$
	$J_c(25 \text{ K}, 0\text{T}) > 5 \times 10^6 \text{ A/cm}^2$
	$J_c(25 \text{ K}, 0\text{T}) > 10^5 \text{ A/cm}^2$
Resistivity Near $T_c$	$\rho(40 \text{ K}) = 0.4\text{--}16 \mu\Omega\text{cm}$
Resistivity Ratio	$RR = \rho(40 \text{ K}) / \rho(300 \text{ K}) = 0.5\text{--}27$
Upper critical fields	$H_{c2}^{ab}(0) = 14\text{--}39 \text{ T}$
	$H_{c2}^c(0) = 2\text{--}24 \text{ T}$
Lower Critical Field	$H_{c1}(0) = 27\text{--}48 \text{ mT}$

## REFERENCES

- J.S. Ahn, E.J. Choi, Carbon substitution effect in MgB<sub>2</sub>, con-mat/0103169 (2001)
- J.M. An, W.E. Pickett, Phys.Rev.Lett. **86**, (2001), 4366.
- S.J. Balaselvi, A. Bharathi, V. S. Sastry, G.L.N. Reddy and Y.Hariharan, Effect of electron and hole doping on the superconducting and normal state properties, cond-mat/0209200, (2002).
- C. Beneduce, H.L. Suo, N. Musolino, and R. Flükiger, Transport critical current densities and n factors in mono- and multifilamentary MgB<sub>2</sub>/Fe tapes and wires using fine powders, cond-mat/0203114, (2002).
- D. J. Bishop et al., Scientific American, **268** (2), (1993), 48
- G. Brumfiel, Superconducting Serendipity in MgB<sub>2</sub>, Focus, (2001)  
<http://focus.aps.org/story/v8/st2>
- C. Buzea, T. Yamashita, Review of superconducting properties of MgB<sub>2</sub>, cond-mat/0108265, to appear in Superconducting Science and Technology, (2001).
- M. R. Cimberle, M. Novak, P. Manfrinetti, A. Palenzona, Magnetic characterization of sintered MgB<sub>2</sub> samples: effect of the substitution or “doping” with Li, Al and Si, cond-mat/0105212, (2001).
- Y.X Chen, D.X Li, G.D Zhang, Microstructural studies of in-situ formed MgB<sub>2</sub> Phases in a Mg alloy matrix composites. Material Science Engineering A, **337**, (2002), 222-227.

H.J Choi, D.Roundary, H. Sun, M.L. Cohen, & S.G. Loule, First principle calculation of superconducting transition in  $MgB_2$  with in the anisotropic Eliashberg formalism. Phys.Rev.B **66**, (2002a), 020513-1 -- 020513-4 66 (2002a).

H.J Choi, D.Roundary, H. Sun, M.L. Cohen, & S.G. Loule, The origin of the anomalous superconducting properties of  $MgB_2$ . Nature **418**, (2002b), 758-760.

DDA, Department of Defense Hand Book of United States of America, Composite Materials Handbook, Vol4 (1999).

C. Dong, J. Y. Xiang, and Z.X. Zhao, Superconductivity and Aluminum Ordering in  $Mg_{1-x}Al_xB_2$  J.Q.Li, L. Li, F.M.Liu cond-mat/0104320 (2001).

D. C. Dunand(a), Superconducting Mg- $MgB_2$  and Related Metal Composites and Methods of Preparation  
<http://www.northwestern.edu/ttp/technology/abstracts/21029.html>.

D. C. Dunand, Synthesis of superconducting Mg/ $MgB_2$  composites, Applied Physics Letters, **79**, (2001), 4186-4188.

G. M. Eliashberg, Interactions between electrons and lattice vibrations in a superconductor. Zh.Eksp.Teor.Fiz.38, 966-976 (1960); Sov. Phys. JETP **11**, (1960), 676-702.

Y. Feng, Y. Zhoo, A.K Pradhan, L. Zhou, P.X Zhang, X. H. Liu, P. Ji, S. J Du, C.F.Liu, Wu Y. and N. Koshizuka, Fabrication and superconducting properties of  $MgB_2$  composite wire by PIT method, Superconductors Science and Technology **15**, (2002), 12-15.

J. File and R.G. Mills, Phys.Rev Lett.**10**, (1963), 93.

D. K. Finmore, J.E. Ostenson, S.L. Bud'ko, G. Lapertot, Thermodynamic and Transport Properties of Superconducting  $Mg^{10}B_2$ , Cond-mat/0102114 v1 (2001).

G. Grasso, A. Malagoli, C. Ferdeghini, S. Rancalla, V. Broccini, M.R. Cimberle and A.S. Siri, Appl. Phys. Lett. **79**, (2001), 230.

G. Giunchi, High Density MgB<sub>2</sub> Obtained by Liquid Infiltration, Con-mat 0207488, (2002).

D.G. Hinks, H. Claus, & J.D. Jorgenson, The complex nature of superconductivity in MgB<sub>2</sub> as revealed by the reduced total isotope effect. Nature **411**, (2001), 457-460.

D.G. Hinks, J.D.Jorgensen, H.Zheng, S. Short, Synthesis and Stoichiometry of MgB<sub>2</sub>, cond-mat/0207161 (2002).

S S Indrakanti, V F Nesterenko, M B Maple, N A Frederick, W M Yuhanz and S. Li, Hot isostatic pressing of bulk magnesium diboride: mechanical and superconducting properties, cont-mat/0105485 (2001).

S.Jin, H. Mavoori and R. B. Van Dover, High transport critical current densities in dense, metal clad superconductor wires of MgB<sub>2</sub>, Nature. **411**, (2001), 563.

C. U. Jung, M.S. Park, W. N. Kang, M. S. Kim, K. H. P Kim, S. V. Lee, S. I. Lee, Applied. Physics Lett. **78**, (2001), 4157.

C.U. Jung., H. J. Kim, M.S Park, M.S Kim., J.Y.Kim, Z. Du, S. I.Lee, K.H.Kim, J.B.Betts, M.Jaime, A.H. Lacerda and G.S. Boebinger, Effect of unreacted Mg imprurities on the transport properties of MgB<sub>2</sub>, Physica C **377**, (2002), 21.

W.N. Kang et al.,. cond-mat/01101446 (2001)

V.F. Kresin, S. A Wolf, Fundamentals of Superconductivity, Plenum Press, (1990)

H. Kitaguchi, H. Kumakura, K. Togano, Strain Effect in MgB<sub>2</sub>/Stainless Steel Superconducting Tape, Physica C **363**, (2001), 198-201.

J.Kortus, I.I. Mazin, K.D. Belashchenko, V.P.Antropov, L.L. Boyer, *Physics. Rev. Lett.* **86**, (2001), 4656.

H. Kotegawa, K. Ishida, Y. Kitaoka<sup>1</sup>, T. Muranaka, N. Nakagawa, H. Takagiwa, and J. Akimitsu; Evidence for High-frequency Phonon Mediated S-wave Superconductivity: 11B-NMR Study of Al-doped MgB<sub>2</sub>, con-mat/0201578 (2002)

J.E. Kunzler, E.Buehler, L. Hsu., & J. Wernick, Superconductivity in Nb<sub>3</sub>Sn at high current density in a magnetic field of 88 kgauss. *Phys. Rev. Lett.***6**, (1961), 89-91.

D.C Lerbalestier, A. Gurevich, D. M. Feldmann & A. Polyanskii, *Nature Insight*, **414**, (2001a), 368.

D. C. Lerbalestier, L. D. Cooley, M. O. Rikel, A. A. Polyanskii, J. Jiang, S. Patnaik, X. Y. Cai, D. M. Feldmann, A. Gurevich, A. A. Squitieri, M. T. Naus, C. B. Eom, E. E. Hellstrom, R. J. Cava, K. A. Regan, N. Rogado, M. A. Hayward, T. He, J. S. Slusky, P. Khalifah, K. Inumaru & M. Haas, Strongly linked current flow in polycrystalline forms of the superconductor MgB<sub>2</sub>, *Nature* **410**, (2001b), 186.

S.Y. Li, Y.M. Xiong, W.Q. Mo, R. Fan, C. H. Wang, X.G.Luo, Z.Sun, H.T.Zhang, L.Li, L.Z.Cao, X.H. Chen, Alkali Metal Substitutions effects in Mg<sub>1-x</sub>A<sub>x</sub>B<sub>2</sub>, *Physica C* **363** (2001)

E. Matienez, L.A Angurel, R. Novario, Study Of Ag And Cu/MgB<sub>2</sub> Powder-In-Tube Composite Wires Fabricated By Insitu Reaction At Low Temperatures con-mat./0203464, (2002)

A. Matsumoto, H. Kumakura, H. Kitaguchi, H. Fujii, K. Togano, The annealing effect of MgB<sub>2</sub> superconducting tapes, *Physica C* **382**, (2002), 207-212.

M.J. Mehl, D.A. Papaconstantopoulos, and D.J. Singh, Effects of C, Cu, and Be substitutions in superconducting MgB<sub>2</sub>, *Physical Review B*, **64**, (2001), 14059(R).

Y. Moritomo, Sh. Xu, Effect of transition metal doping in MgB<sub>2</sub> superconductor, cond-mat 0104568 (2001)

S. Murase, K. Itoh, H.Wada, K.Noto, Y.Kimura, Y. Tanaka and K. Osamura, Critical temperature measurement methods of composite superconductors., Physca C **357-360**, (2001), 1197-1200.

J. Namatsu, N.Nakgawa, T.Muranaka, Y.Zenitani and J. Akimitsu, Nature **410**, (2001), 63-64.

Kamerling H. Onnes, Lerden Commun,124c (1911)

R. Osborn, E. A. Goremychkin, A. I. Kolesnikov and D. G. Hinks Phys. Rev. Lett. **87**, (2001), 017005.

M. Paranthaman, J.R. Thompson, and D.K. Christen, Effect Of Carbon-Doping In Bulk Superconducting MgB<sub>2</sub> Samples, Submitted to Physica C (2001)

T.A. Prikha, W. Gawalek, A.B. Surzhenko, V.E. Moshchil, N. V. Sergienko, Ya.M. MoSavchuk, V.S. Melnikov, P.A. Nagorny, T. Habisreuther, S.N. Dub, M. Wendth, D. Litzkendorf, J. Dellith, Ch. Schmidh, G. Krabbes, and A. V Vlasenko. High-pressure synthesis of MgB<sub>2</sub> with and with out tantalum addition, Physica C **372-376** (2002).

R.A. Ribeiro, S.L, Budiko, C. Petrovic, P.C. Canfield, Effects of stoichiometry, purity, etching and distilling on resistance of MgB<sub>2</sub> pellets and wire segments, Physica C **382**, (2002), 194-202.

S. I. Schlacher, W. Goldacker, J. Reiner, S. Zimmer, B. Liu, and B. Obst, Influence of the preparation Process on microstructure, Critical Current Density and T<sub>c</sub> of MgB<sub>2</sub> Powder-in-Tube Wires., cond-mat/0210591 (2002).

A. Sharoni, O. Millo, G. Letius, S. Reich J. Phys., Spatial variations of the superconductor gap structure in MgB<sub>2</sub>/Al composites, Condens Matter **13**, (2001), L503.

T.C. Shields, K. Kawano, D Holdom and J.S Abell, Microstructure and superconducting properties of hot isostatically pressed MgB<sub>2</sub>. *Superconducting Science and Technology* **15**, (2002), 202-205.

J.S. Slusky, N. Rogado, K.A. Regan, M.A. Hayward, P. Khalifah, T. He, K. Inumaru, S. Loureiro, M.K Haas, H.W Zandbergen, R.J. Cava, cond-mat/0102262 (2001)

J.S. Slusky et al., Loss of superconductivity with the addition of Al to MgB<sub>2</sub> and a structural transition in Mg<sub>1-x</sub>AlB<sub>2</sub>. *Nature* **410**, (2001), 343-345.

K.J. Song, N. J. Lee, H. M. Jang, H.S. Ha, D.W. Ha, S. S. Oh, M.H. Sohn, R.K. Ka, C. Park, Y. K. Kwan, K.S. Ryu, Single filament composite MgB<sub>2</sub>/stainless-steel ribbons by powder-in-tube process. *Physica C* **370**, (2002), 21-26.

H.L. Suo, P. Lezza, D. Uglietti, C. Beneduce, V. Abacherli and R. Flukiger, Transport Critical Current Densities And N Factors In Mono- And Multifilamentary MgB<sub>2</sub>/Fe Tapes And Wires Using Fine Powders. Cond-mat/0208133 (2002).

S. Soltaian, X. L. Wang, J. Horvat, A.H. Li, H.K. Liu, S.X. Dou, Improvements of critical current density in the Cu/MgB<sub>2</sub> and Ag/MgB<sub>2</sub> superconducting wires using the fast formation method. *Physica C* **382** (2002).

K. Tachikawa, Y. Yamada, O. Suziki, M. Enomoto, M. Aodai, Effect Of Metal Powder Addition On The Critical Current In MgB<sub>2</sub> Tapes, *Physica C* **382**, (2002), 108-112.

J.R. Thompson. M. Parantaman, D.K. Christen, K.d. Sorge, H.J. Kim, J.G. Ossandan, *Supercond. Sci. Technol.*, **14**, (2001), L19.

A. Tampieri, G. Celotti, S. Sprio, D. Rinaldi, G. Barucca, R. Caciuffo, Effects of copper doping in MgB<sub>2</sub> superconductor, *Solid state communications*, **121**, (2002), 497-500.

M. Tinkham, *Introduction to superconductivity*, McGraw-Hill, New York, 1975.

- J.Tallon, Industry warms to superconductors, *Physics World*, **27**, (2001), 31.
- T. Yildirim, O. Gülseren, J. W. Lynn, C. M. Brown, T. J. Udovic, Q. Huang, N. Rogado, K. A. Regan, M. A. Hayward, J. S. Slusky, T. He, M. K. Haas, P. Khalifah, K. Inumaru, and R. J. Cava Giant, Anharmonicity and Nonlinear Electron-Phonon Coupling in MgB<sub>2</sub>: A Combined First-Principles Calculation and Neutron Scattering Study, *Phys. Rev. Lett.*, **87**, (2001), 037001.
- Wu, M. K. et al., Superconductivity at 93 K in a new mixed-phase Y-Ba-Cu-O compound system at ambient pressure. *Phys. Rev. Lett.*, **58**, (1987), 908–912.
- S. Xu, Y. Moritomo, K. Kato and A. Nakamura, Mn- substitution effects on MgB<sub>2</sub> superconductors, *J. Phys. Soc. Jpn.*, **70**, (2001), 1889-1891.
- MY. G. Zha, X.P.Zhang, P.T.Qiao, H.T.Zhang, S.L.Jia, B.S.Cao, M.H.Zhu, Z.H.Han, X.L.Wang, B.L.Gu, Effects of Li Doping on Structure and Superconducting Transition Temperature of Mg<sub>1-x</sub> A<sub>x</sub>B<sub>2</sub>. *Physica C*, **361**, (2001), 91-94.
- Y. Zhoa, Y.Feng, D.X. Huong, T. Machi, C.H.Cheng, K. Nakao, N. Chikumoto, Y. Fudamoto, N. Kashizuka, M. Murakami, Doping effects of Zr and Ti on the Critical Current Density of MgB<sub>2</sub> Bulk Superconductors Prepared under ambient pressure, *Physica C*, **378-381**, (2002), 122-126.
- Y. Zhoa, Y.Feng, C.H. Cheng, L. Zhou, Y. Wu, T. Machi, Y. Fudomoto, N.Koshizuka, and M. Murakami, High critical current density of MgB<sub>2</sub> bulk superconductor doped with Ti sintered at ambient pressure, *Applied Physics Letters*, **79**, (2001), 8.
- S. Zhou, A. V. Pan, M. Ionescu, H. Liu and S. Dou, Influence of Ag, Cu and Fe sheaths on MgB<sub>2</sub> Superconducting Tapes, *Superconductor Science and Tecnology*, **15**, (2002), 236-240.